

Washington University School of Medicine Digital Commons@Becker

Open Access Publications

2018

Engineered dengue virus domain III proteins elicit cross-neutralizing antibody responses in mice

Julia C. Frei

Albert Einstein College of Medicine

Ariel S. Wirchnianski

Albert Einstein College of Medicine

Jennifer Govero

Washington University School of Medicine in St. Louis

Olivia Vergnolle

Albert Einstein College of Medicine

Kimberly A. Dowd

National Institutes of Health

See next page for additional authors

Follow this and additional works at: https://digitalcommons.wustl.edu/open_access_pubs

Recommended Citation

Frei, Julia C.; Wirchnianski, Ariel S.; Govero, Jennifer; Vergnolle, Olivia; Dowd, Kimberly A.; Pierson, Theodore C.; Kielian, Margaret; Girvin, Mark E.; Diamond, Michael S.; and Lai, Jonathan R., "Engineered dengue virus domain III proteins elicit cross-neutralizing antibody responses in mice." *Journal of Virology*.92,18. e01023-18. (2018).
https://digitalcommons.wustl.edu/open_access_pubs/7088


This Open Access Publication is brought to you for free and open access by Digital Commons@Becker. It has been accepted for inclusion in Open Access Publications by an authorized administrator of Digital Commons@Becker. For more information, please contact engeszer@wustl.edu.

Authors

Julia C. Frei, Ariel S. Wirchnianski, Jennifer Govero, Olivia Vergnolle, Kimberly A. Dowd, Theodore C. Pierson, Margaret Kielian, Mark E. Girvin, Michael S. Diamond, and Jonathan R. Lai



Engineered Dengue Virus Domain III Proteins Elicit Cross-Neutralizing Antibody Responses in Mice

Julia C. Frei,^a Ariel S. Wirchnianski,^a Jennifer Govero,^b Olivia Vergnolle,^a Kimberly A. Dowd,^f Theodore C. Pierson,^f
 Margaret Kielian,^c Mark E. Girvin,^a Michael S. Diamond,^{b,d,e} Jonathan R. Lai^a

^aDepartment of Biochemistry, Albert Einstein College of Medicine, Bronx, New York, USA

^bDepartment of Medicine, Washington University in St. Louis School of Medicine, St. Louis, Missouri, USA

^cDepartment of Cell Biology, Albert Einstein College of Medicine, Bronx, New York, USA

^dDepartment of Molecular Microbiology, Washington University in St. Louis School of Medicine, St. Louis, Missouri, USA

^eDepartment of Pathology and Immunology, Washington University in St. Louis School of Medicine, St. Louis, Missouri, USA

^fViral Pathogenesis Section, National Institute of Allergy and Infectious Diseases, National Institutes of Health, Bethesda, Maryland, USA

ABSTRACT Dengue virus is the most globally prevalent mosquito-transmitted virus. Primary infection with one of four cocirculating serotypes (DENV-1 to -4) causes a febrile illness, but secondary infection with a heterologous serotype can result in severe disease, due in part to antibody-dependent enhancement of infection (ADE). In ADE, cross-reactive but nonneutralizing antibodies, or subprotective levels of neutralizing antibodies, promote uptake of antibody-opsonized virus in Fc- γ receptor-positive cells. Thus, elicitation of broadly neutralizing antibodies (bNAbs), but not nonneutralizing antibodies, is desirable for dengue vaccine development. Domain III of the envelope glycoprotein (EDIII) is targeted by bNAbs and thus is an attractive immunogen. However, immunization with EDIII results in sera with limited neutralization breadth. We developed “resurfaced” EDIII immunogens (rsDIIIs) in which the A/G strand epitope that is targeted by bNAbs is maintained but less desirable epitopes are masked. RsDIIIs bound 4E11, but not serotype-specific or nonneutralizing antibodies. One rsDIII and, unexpectedly, wild-type (WT) DENV-2 EDIII elicited cross-neutralizing antibody responses against DENV-1 to -3 in mice. While these sera were cross-neutralizing, they were not sufficiently potent to protect AG129 immunocompromised mice at a dose of 200 μ l (50% focus reduction neutralization titer [FRNT₅₀], ~1:60 to 1:130) against mouse-adapted DENV-2. Our results provide insight into immunogen design strategies based on EDIII.

IMPORTANCE Dengue virus causes approximately 390 million infections per year. Primary infection by one serotype causes a self-limiting febrile illness, but secondary infection by a heterologous serotype can result in severe dengue syndrome, which is characterized by hemorrhagic fever and shock syndrome. This severe disease is thought to arise because of cross-reactive, non- or poorly neutralizing antibodies from the primary infection that are present in serum at the time of secondary infection. These cross-reactive antibodies enhance the infection rather than controlling it. Therefore, induction of a broadly and potently neutralizing antibody response is desirable for dengue vaccine development. Here, we explore a novel strategy for developing immunogens based on domain III of the E glycoprotein, where undesirable epitopes (nonneutralizing or nonconserved) are masked by mutation. This work provides fundamental insight into the immune response to domain III that can be leveraged for future immunogen design.

Received 12 June 2018 Accepted 29 June 2018

Accepted manuscript posted online 5 July 2018

Citation Frei JC, Wirchnianski AS, Govero J, Vergnolle O, Dowd KA, Pierson TC, Kielian M, Girvin ME, Diamond MS, Lai JR. 2018. Engineered dengue virus domain III proteins elicit cross-neutralizing antibody responses in mice. *J Virol* 92:e01023-18. <https://doi.org/10.1128/JVI.01023-18>.

Editor Terence S. Dermody, University of Pittsburgh School of Medicine

Copyright © 2018 American Society for Microbiology. All Rights Reserved.

Address correspondence to Jonathan R. Lai, jon.lai@einstein.yu.edu.

KEYWORDS dengue virus, domain III, immunogen, phage display, protein engineering, vaccine

Dengue virus (DENV) is a member of the family *Flaviviridae* and is related to other globally important pathogens, such as yellow fever (YFV), West Nile (WNV), and Zika (ZIKV) viruses. Annually, there are an estimated 390 million DENV infections, with a case fatality rate of <1% (1, 2). There are four serotypes of DENV (DENV-1 to -4), which cocirculate in regions of endemicity and are transmitted by *Aedes aegypti* and *Aedes albopictus* mosquitoes (1, 3). Primary infection with DENV often results in a self-limited febrile illness, with lifelong immunity established against the infecting serotype and transient (e.g., approximately 6-month) cross-protection against the other three serotypes. After cross-protection wanes, a secondary infection with a different serotype can result in severe dengue syndrome, which is characterized by vascular leakage, bleeding, and hypotensive shock (4, 5). This enhancement during secondary DENV exposure is due, in part, to antibody-dependent enhancement of infection (ADE). ADE is a phenomenon in which antibodies that arise during the primary infection are cross-reactive with the heterologous serotypes and thus bind to the virus but are nonneutralizing. Antibody-coated virus particles are more readily internalized by Fc γ receptor-positive myeloid cells, resulting in increased infection, viremia, and proinflammatory cytokine production, which ultimately lead to severe disease (5–7). Thus, it is considered highly desirable for DENV vaccines to elicit balanced and broadly neutralizing antibody responses against all four serotypes to minimize the possibility of ADE (5, 8).

A safe and effective DENV vaccine is a high global priority (9). Sanofi Pasteur licensed the first DENV vaccine; CYD-17D (Dengvaxia) is a chimeric, live-attenuated, tetravalent vaccine in which the glycoproteins of each DENV serotype are cloned in a backbone of the YFV 17D vaccine strain genome (10). The overall efficacy of CYD-17D was demonstrated to be approximately 60%; however, the efficacy against each serotype varied and was particularly low for DENV-2 (11, 12). CYD-17D efficacy depends on the DENV immune status prior to vaccination, with seronegative patients demonstrating much lower protective efficacy than seropositive patients (8, 10, 13). Indeed, recently published data from the phase 4 postmarketing study of CYD-17D revealed greater symptomatic DENV disease in a minority of naive individuals who were vaccinated and subsequently naturally infected (14, 15). Another live-attenuated tetravalent vaccine candidate, TV005, was recently shown to induce high levels of neutralizing antibody against all four serotypes in phase 2 trials, although it is currently unknown how sustained these titers will be over time (16).

Protein immunogens consisting of antigenic regions of the DENV glycoprotein E, which coat the mature virion and are the dominant targets of neutralizing antibodies, present an attractive alternative approach for vaccine discovery (17). Prefusion E exists as a homodimer and contains three ectodomains: domain I (EDI) serves as a molecular hinge between domains II and III (EDII and EDIII), EDII is the dimerization domain and contains the fusion loop at its distal end, and EDIII is an Ig-like domain implicated in binding host cell surface receptors (Fig. 1A) (18–20). Antibodies targeting the highly conserved fusion loop in EDII have broad cross-reactivity but variable neutralizing potentials (21), with the exception of the highly neutralizing E dimer epitope antibodies, which recognize a quaternary epitope that includes the fusion loop (22, 23).

EDIII is a target of many antibodies, including serotype-specific neutralizing monoclonal antibodies (MAbs), such as 3H5, which binds the lateral ridge/FG loop, and cross-reactive, nonneutralizing MAbs, such as 2H12 and WNV-E111, that bind the AB loop, as well as broadly neutralizing antibodies (bNAbs), such as 4E11 and 1A1D-2, that engage a discontinuous epitope encompassing residues of the A and G strands (24–32). Both 4E11 and 1A1D-2 (both murine) bind and neutralize DENV-1 to -3 strongly, with 4E11 showing additional modest inhibitory activity against DENV-4 (25, 27, 33). Structural studies of 1A1D-2 and 4E11 in complex with EDIII indicated that the difference in neutralization breadth of these two MAbs was due to a shift in the epitope on EDIII,

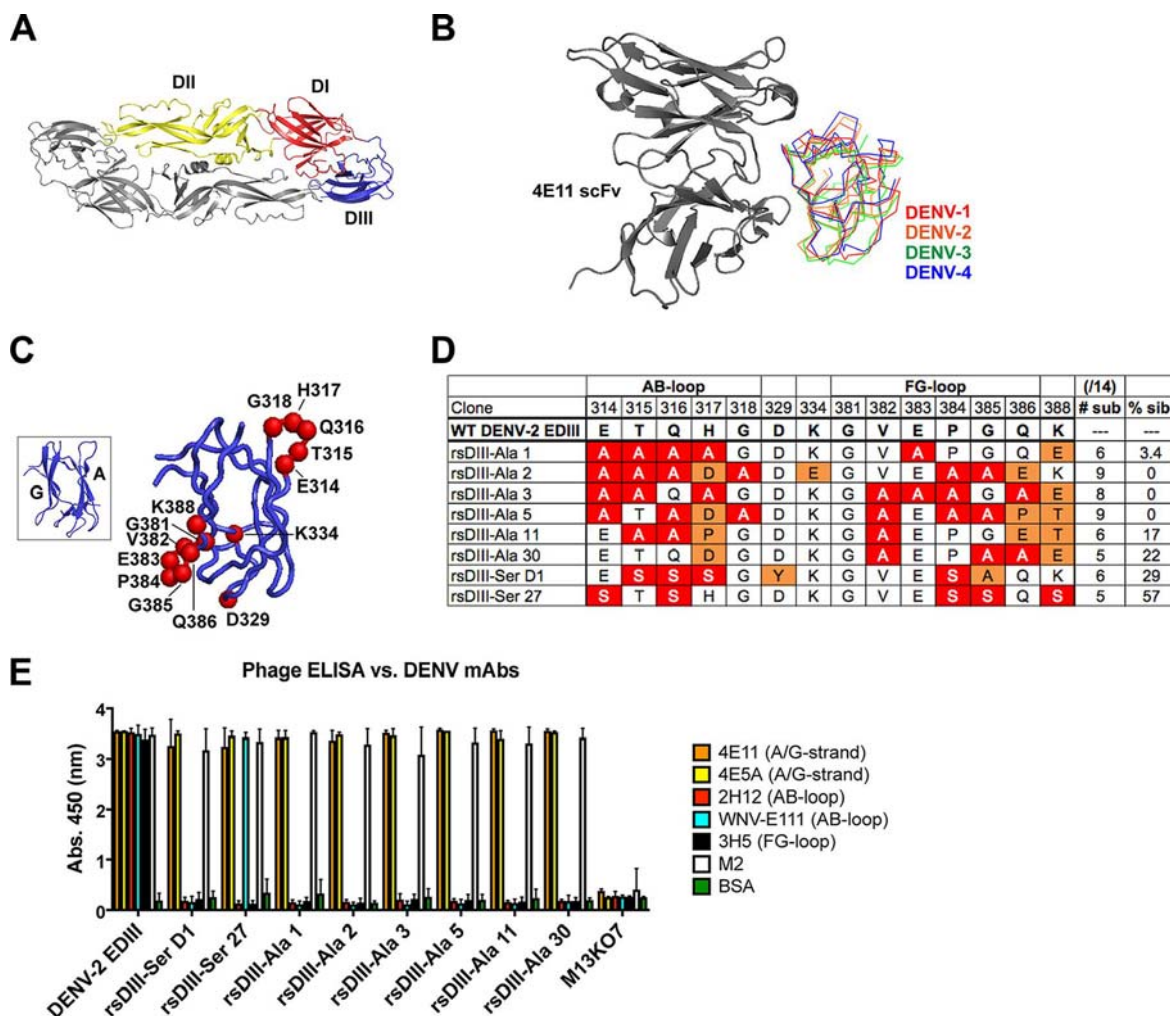


FIG 1 Rs-DIIIs demonstrate favorable binding to DENV MAbs. (A) Domain organization of prefusion homodimeric E glycoprotein. One subunit is color coded by domain (ED I, red; ED II, yellow; and ED III, blue); the other subunit is shown in gray. DENV-2 is shown as an example from Protein Data Bank (PDB) ID 1OAN (19). (B) Overlay of DENV-1 to -4 EDIIIs bound to the single-chain variable fragment (scFv) of 4E11 from PDB ID 3UZO, 3UZY, 3UZE, and 3UYF (27). (C) The red spheres indicate library positions on DENV-2 EDIII that were allowed to vary in phage libraries (PDB ID 3UZY [27]). The inset shows the orientation of EDIII, with the A and G strands highlighted. (D) Sequence of rsDIII at the randomized positions. Red indicates substitutions with alanine or serine, and orange indicates other possible substitutions. (E) Reactivity profiles of phage expressing WT DENV-2 EDIII and rsDIIIs toward a panel of DENV MAbs: 2H12 and WNV-E111 (AB loop), 3H5 (FG loop), and M2 (FLAG). Wells coated with BSA served as a negative control. The data are from two experiments performed in duplicate and are plotted as means and standard deviations (SD).

with the 1A1D-2 epitope shifted toward the A strand and the 4E11 epitope centered over the A/G strands (Fig. 1B). 4E11 was subsequently engineered to bind with higher affinity to DENV-4 EDIII and showed 75-fold higher neutralization potency than the parent MAb (28). Further optimization of 4E11 for binding to DENV-4 resulted in a variant termed Ab513, which had increased affinity for DENV-3 and DENV-4 EDIII and increased neutralization potency and breadth and protected mice against viremia, thrombocytopenia, and vascular leakage (34).

Because EDIII is targeted by bNAbs and can be expressed as an independent, soluble domain, it has received attention as a potential immunogen. However, previous immunization studies of mice and nonhuman primates with EDIII-containing proteins have shown that, while a robust antibody response against EDIII is elicited, neutralization is modest and limited to serotype-specific responses (35–45). The limited neutralization potential of EDIII antisera may be due to the presence of antibodies that target the immunodominant AB loop epitope; such antibodies are cross-reactive but largely nonneutralizing (26, 46). 2H12, a prototypical AB loop antibody, demonstrates sub-

nanomolar affinity for soluble EDIII but cannot bind the virus at sufficient occupancy for neutralization, likely because the AB loop epitope is largely cryptic and only occasionally exposed during viral “breathing” (47). The AB loop is largely conserved across flaviviruses, and thus, some WNV MAbs (e.g., WNV-E111) cross-react with DENV (26). Similar to other flaviviruses, DENV also contains the lateral-ridge epitope (LR), which includes parts of the N terminus (A strand) and BC, DE, and FG loops (26, 31, 48). MAbs to DENV LR, such as 3H5, are potently neutralizing but serotype specific and cannot broadly neutralize DENV infection (26, 49, 50). An ideal EDIII-based immunogen would capture the properties of the A/G strand epitope, but not the AB loop (nonneutralizing) or FG loop (serotype-specific) epitopes.

“Epitope-focusing” or “resurfacing” approaches, where critical neutralizing epitopes are emphasized but nonneutralizing or undesirable epitopes are masked by mutation, represent a promising platform for optimizing protein immunogens (51–53). Resurfacing strategies have been used recently to optimize immunogens for influenza virus, respiratory syncytial virus, and human immunodeficiency virus type 1 (HIV-1) (51, 54–56). In general, resurfacing strategies involve identification of protein variants in which undesirable epitopes are mutated to residues that do not perturb the global structure of the antigen (so as not to destroy desired epitopes) but provide remodeling of the undesirable epitopes. While such a procedure may not guarantee that antibody responses will be focused on the desirable epitope, any immune response against the engineered regions of the resurfaced antigen would target sequences that are not homologous to the authentic virus. Thus, a memory B cell response to these regions would not be elicited during natural infection. Resurfacing by mutation to amino acids that are statistically disfavored in antibody-antigen interactions, such as alanine or serine (57), may be advantageous for diverting immune responses away from particular nonprotective epitopes and warrants investigation.

Using structure-guided design and phage display, we engineered a panel of DENV-2-based resurfaced EDIIIs (rsDIIIs) in which cross-reactive, nonneutralizing (AB loop) and serotype-specific (FG loop/lateral-ridge) epitopes were “hidden” via mutation to alanine or serine. Our rsDIIIs showed decreased binding to antibodies targeting unfavorable epitopes while maintaining high affinity for the broadly neutralizing antibodies, 4E11 and 4E5A (A/G strand binders). Upon immunization in mice, one rsDIII (rsDIII-Ala30), as well as wild-type (WT) DENV-2 EDIII, elicited broadly reactive and cross-neutralizing antibody responses. The elicitation of cross-neutralizing sera by WT DENV-2 EDIII was unexpected, given previous reports of homotypic response upon immunization with WT EDIII (35, 36, 41, 42, 58). Together, these results indicate that methods of immunogen design, preparation, and loop configuration may influence neutralization breadth. Although the sera induced by WT DENV-2 EDIII and rsDIII-Ala30 were broadly neutralizing, they were not sufficient to protect highly vulnerable immunocompromised AG129 mice from lethal DENV-2 challenge after passive transfer at a dose of 200 μ l (50% focus reduction neutralization titer [FRNT₅₀], \sim 1:60 to 1:130). These results indicate that induction of a cross-neutralizing response is possible with designed EDIII variants but that potency must be increased for protective effect.

RESULTS

RsDIIIs maintain the A/G strand epitope but have remodeled AB and FG loops.

Our objective was to develop EDIII variants in which the A/G strand that is targeted by the bNAb 4E11 was maintained but other regions—such as the AB loop that is targeted by nonneutralizing MAb 2H12 or the FG loop that is targeted by type-specific DENV-2 MAb 3H5—were masked by mutation. Phage display coupled with structure-guided design provides an efficient strategy for protein or antibody optimization, and we and others have previously demonstrated that EDIIIs from all four DENV serotypes can be expressed efficiently on the M13 bacteriophage as a platform for engineering (59–62).

The DENV-2 EDIII (Jamaica/1409/1983) sequence (residues 296 to 400) was expressed as a fusion to the minor pIII coat protein with an N-terminal FLAG tag, as previously reported (59). Resurfacing phage libraries were constructed with targeted

variation in the AB (residues 314 to 318; a cross-reactive, nonneutralizing epitope) and FG (residues 381 to 386; a serotype-specific epitope) loops on DENV-2 EDIII. Furthermore, a surface accessibility analysis was performed using AREAIMOL and a probe sphere of 1.4 Å, and “surface-exposed” residues were defined as those containing an atom with an accessible surface area greater than 45 Å² (63, 64). Based on this analysis, surface-exposed, hydrophilic D329, K334, and K388 also were varied in the resurfacing libraries; hydrophilic residues were targeted because they are enriched in epitopes (57),

Two libraries were constructed in which randomized positions were allowed to vary in a restricted manner between the WT residue identity and alanine (rsDIII-Ala library) or serine (rsDIII-Ser library) (Fig. 1C). Due to the degeneracy of the genetic code, in some cases, a third or fourth residue was also permitted in both libraries. Alanine was chosen as a substitution because it is underrepresented in antibody-antigen interfaces (57), and serine was chosen because the hydroxyl-containing side chain is relatively inert and thus unlikely to mediate the long-range or hydrophobic interactions typically required for antibody-antigen binding (65). DENV-2 was chosen as the EDIII scaffold, as CYD-17D demonstrated the lowest efficacy against serotype 2. Libraries were synthesized using mutagenesis and degenerate primers (see Materials and Methods) (66). The final library sizes were 1×10^9 and 2.5×10^9 transformants for the alanine and serine libraries, respectively. Both library sizes were at least 100-fold larger than their calculated theoretical diversities (5.2×10^5 and 1.7×10^7 , respectively), indicating adequate coverage of the sequence space.

Both libraries were subjected to selection and screening against bNAb 4E11. The rsDIII-Ala library selection resulted in the isolation of 32 unique EDIII variants; six of these clones were chosen for further characterization based on the number of mutations relative to the WT and the frequency of the sequence in the enzyme-linked immunosorbent assay (ELISA)-positive pool (number of siblings) (Fig. 1D). Screening of the rsDIII-Ser library was less efficient, with only four unique sequences isolated (Fig. 1D). Sequences of both the AB and FG loops were highly mutated in rsDIIIs from the eight final candidates.

To examine if AB and FG loop epitopes were sufficiently masked in rsDIIIs, single-endpoint phage ELISA experiments were conducted with MAbs 2H12 and WNV-E111 (AB loop specific) and 3H5 (FG loop specific) with all eight phage-expressed clones, as well as WT DENV-2 EDIII-expressing phage (Fig. 1E). Wild-type M13KO7 helper phage, which do not express a fusion protein, were included as a negative control. All phage clones bound with comparable reactivities to MAb M2, which binds to the N-terminal FLAG tag (DYKDDDDK), indicating there were no large differences in phage expression among rsDIIIs and WT DENV-2 EDIII. As expected, WT DENV-2 EDIII-displaying phage bound to 4E11 and 4E5A (A/G strand specific), 2H12, WNV-E111, 3H5, and M2, but not the negative control, bovine serum albumin (BSA). The rsDIII-displaying phage demonstrated reactivity with 4E11, 4E5A, and M2 comparable to that of WT DENV-2 EDIII-expressing phage, whereas rsDIII phage showed minimal binding to 2H12, WNV-E111, and 3H5. These results indicate that the AB and FG loop epitopes were altered to ablate recognition by these prototypic MAbs but that the A/G strand epitope was maintained. Furthermore, the similar M2 reactivities among all the clones suggest that the resurfacing mutations did not affect phage expression levels. RsDIII-Ser27 bound the AB loop antibody WNV-E111 but not 2H12, suggesting that recognition of the WNV-E111 epitope depends on residue H317, which is maintained in rsDIII-Ser27 but not others.

WT DENV-2 EDIII and rsDIIIs were expressed as soluble proteins bearing an N-terminal hexahistidine (His₆) tag and purified under denaturing conditions. Denatured EDIII or rsDIIIs were then oxidatively refolded; rsDIIIs aggregated to varying extents during the refolding. Based on stability and expression yield, rsDIII-Ala11 and rsDIII-Ala30 were chosen for further purification by size exclusion chromatography (SEC) and characterization. After the refolding step, WT DENV-2 EDIII, rsDIII-Ala11, and rsDIII-Ala30 each contained aggregate and monomer peaks by SEC (Fig. 2A); only the monomer fraction was isolated and utilized for subsequent experiments.

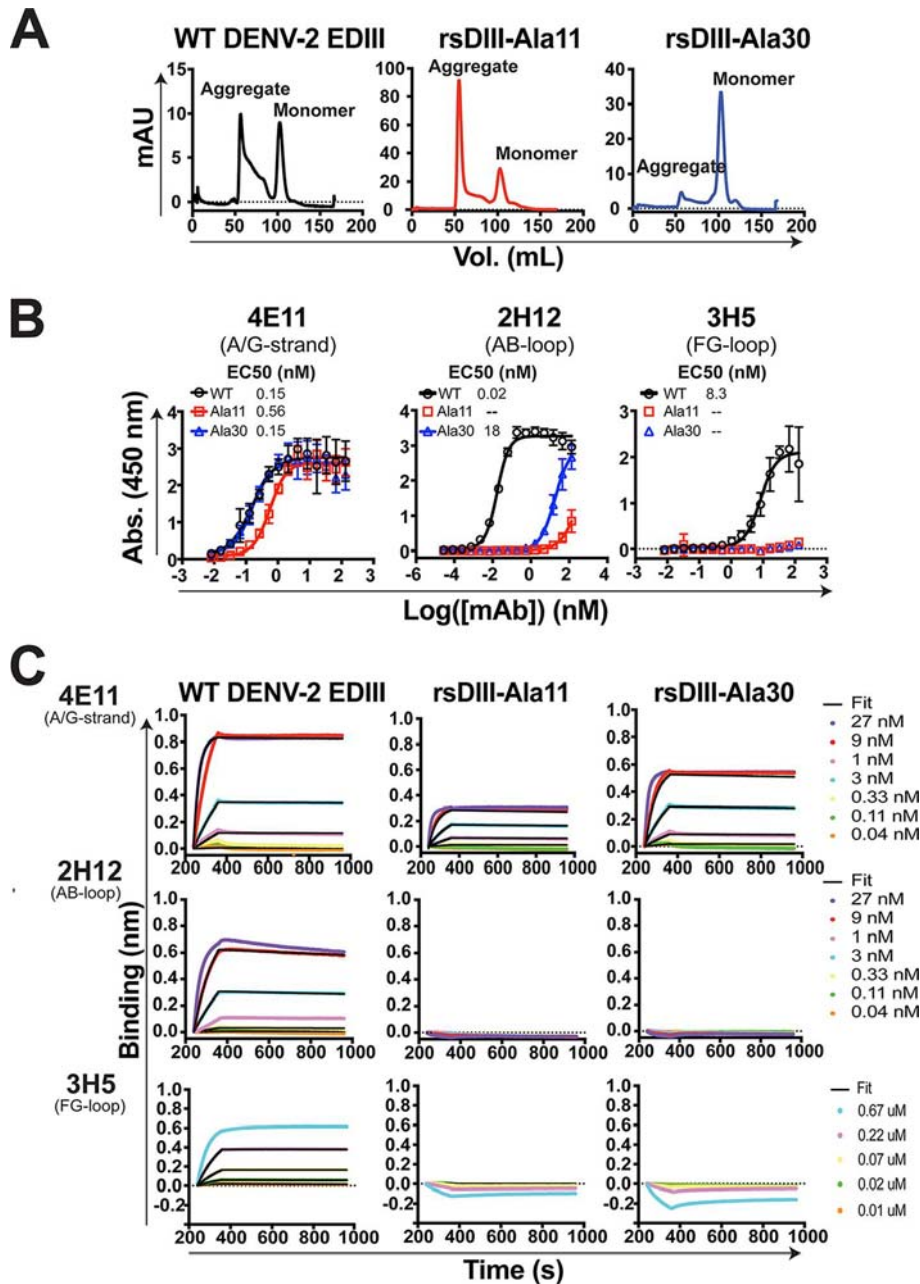


FIG 2 Biochemical characterization of rsDIII variants indicating abolishment of unfavorable epitopes. (A) Size exclusion chromatogram of WT and rsDIII variants indicating two populations of EDIII, aggregated and monomeric. The monomeric fraction was used in further experiments. AU, arbitrary units. (B) RsDIII variants bind only to MAb 4E11 with high affinity and show little or no binding to MAb 2H12 and 3H5 by ELISA. In contrast, WT DENV-2 EDIII binds to all three antibodies. The data are graphed as means \pm SD from the results of two experiments performed in triplicate. Abs., absorbance. (C) RsDIII variants bind only to MAb 4E11 and demonstrate no binding to MAb 2H12 and 3H5 by BLI. RsDIII variants were captured on Ni-NTA sensors, followed by antibody association and dissociation. Antibody concentrations ranged from 27 to 0.01 nM for 4E11 and 2H12 and from 6 to 0.01 μ M for 3H5. The data were fit to a global 1:1 binding model.

Binding profiles for soluble EDIII or rsDIII variants against 4E11, 2H12, and 3H5 were determined initially by ELISA (Fig. 2B). The half-maximal effective concentration (EC₅₀) values for WT DENV-2 EDIII against 4E11, 2H12, and 3H5 were 0.15, 0.017, and 17 nM, respectively. In contrast, rsDIII-Ala11 did not appreciably bind 2H12 or 3H5 but maintained strong reactivity with 4E11 (EC₅₀ = 0.56 nM). RsDIII-Ala30 also maintained avid binding to 4E11 (EC₅₀ = 0.02 nM) and exhibited markedly reduced binding to 2H12 (EC₅₀ = 18 nM) relative to WT DENV-2 EDIII (EC₅₀ = 0.017 nM), and only weak reactivity

toward 3H5 at high concentration. Thus, the reactivity profiles of the purified proteins were similar to that observed by phage ELISA, with WT DENV-2 EDIII binding all the MABs but rsDIII-Ala11 and rsDIII-Ala30 displaying reduced or ablated avidity toward AB and FG loop MABs.

Interactions of WT DENV-2 EDIII, rsDIII-Ala11, and rsDIII-Ala30 with the panel of MABs were further characterized by biolayer interferometry (BLI) (Fig. 2C). EDIIIs were immobilized on nickel-nitrilotriacetic acid (Ni-NTA) biosensors, followed by MAB association and dissociation. Analysis in this format precludes definitive determination of the dissociation constant (K_D), due to the potential of bivalent antibody “walking” along the matrix of epitopes on the sensor (67). Nonetheless, association and dissociation kinetics could be derived for comparative analysis (Table 1). The BLI data were consistent with the ELISA data and indicated that rsDIIIs maintained affinity for bNAb 4E11 that was comparable to that of WT DENV-2 EDIII, with markedly reduced binding to 2H12 and 3H5. Together, the data confirm that the conformational integrity of the A/G strand epitope is maintained in rsDIII-Ala11 and rsDIII-Ala30 but that AB and FG loops are altered. The alternative BLI format, in which the MAB was bound to the sensor, followed by association and dissociation of monovalent EDIII or rsDIIIs, yielded consistently low signal-to-noise sensorgrams, for unclear reasons.

To determine if rsDIII mutations perturbed the core EDIII Ig-like fold, two-dimensional ^{15}N - ^1H heteronuclear single quantum coherence (HSQC) spectra of ^{15}N -labeled rsDIII-Ala11, rsDIII-Ala30, and WT DENV-2 EDIII were collected (Fig. 3A). Peak assignments for WT DENV-2 EDIII were completed using data collected from three-dimensional (3D) experiments on a ^{15}N - ^{13}C -double-labeled sample. Peak assignments closely matched previously published DENV-2 EDIII assignments (68). The ^{15}N - ^1H HSQC spectra of rsDIIIs were similar to that of WT DENV-2 EDIII and contained well-dispersed chemical shifts (see Table S1 in the supplemental material). Resonances that corresponded to core residues on WT DENV-2 EDIII overlapped with resonances in rsDIII-Ala11 or rsDIII-Ala30 (Fig. 3B; colored red and blue, respectively), indicating that the introduced mutations did not grossly alter the core fold.

rsDIIIs elicit broadly reactive and cross-neutralizing antibodies *in vivo*. To test the immunogenicity of engineered rsDIIIs, groups of 10 female, 6-week-old BALB/c mice were immunized with either rsDIII-Ala11 or rsDIII-Ala30 on days 0, 14, and 28. Immunogens were administered by an intraperitoneal (i.p.) route in complete Freund’s adjuvant (CFA) on day 0 and in incomplete Freund’s adjuvant (IFA) for boosting. In addition, our own preparation of WT DENV-2 EDIII was included as a control to benchmark with previous studies (35, 36, 40). Endpoint antibody titers were determined by serum ELISA against the respective immunogen (Fig. 4B, top). All of the mice exhibited robust immunogen-specific antibody responses after two immunizations (endpoint titers, $\sim 1:10^5$), and the titers remained relatively constant between days 28 and 90. The antibody responses were not directed at the hexahistidine tag (His tag), as none of the samples bound to an unrelated His-tagged protein, the Sudan virus glycoprotein (GP_{SUDV}) (Fig. 4B, bottom). To assess cross-reactivity, the sera of five representative mice from each group were tested by ELISA against purified EDIIIs from DENV-1 to -4 (Fig. 4C). In all cases, the sera were broadly cross-reactive for EDIIIs from all four serotypes.

To determine the functional activities of the serum antibodies, focus reduction neutralization tests (FRNTs) were conducted against all four serotypes of DENV with sera from days 60 and 90. Naive sera showed no neutralization activity against DENV-1 to -3 but demonstrated inhibitory activity at higher concentrations against DENV-4, potentially due to nonspecific virus blocking or natural antibodies; thus, it was difficult to determine the immunogen-specific neutralizing titers against DENV-4. Unexpectedly, given prior studies showing that WT EDIII was inefficient at generating bNAbs (35, 36, 41, 42, 58), we found that sera from WT DENV-2 EDIII-immunized mice demonstrated neutralizing activity against DENV-1 to -3 with half-maximal inhibitory concentration (IC_{50}) titers of 1:270, 1:190, and 1:280, respectively (Fig. 5A). Sera from rsDIII-Ala30-

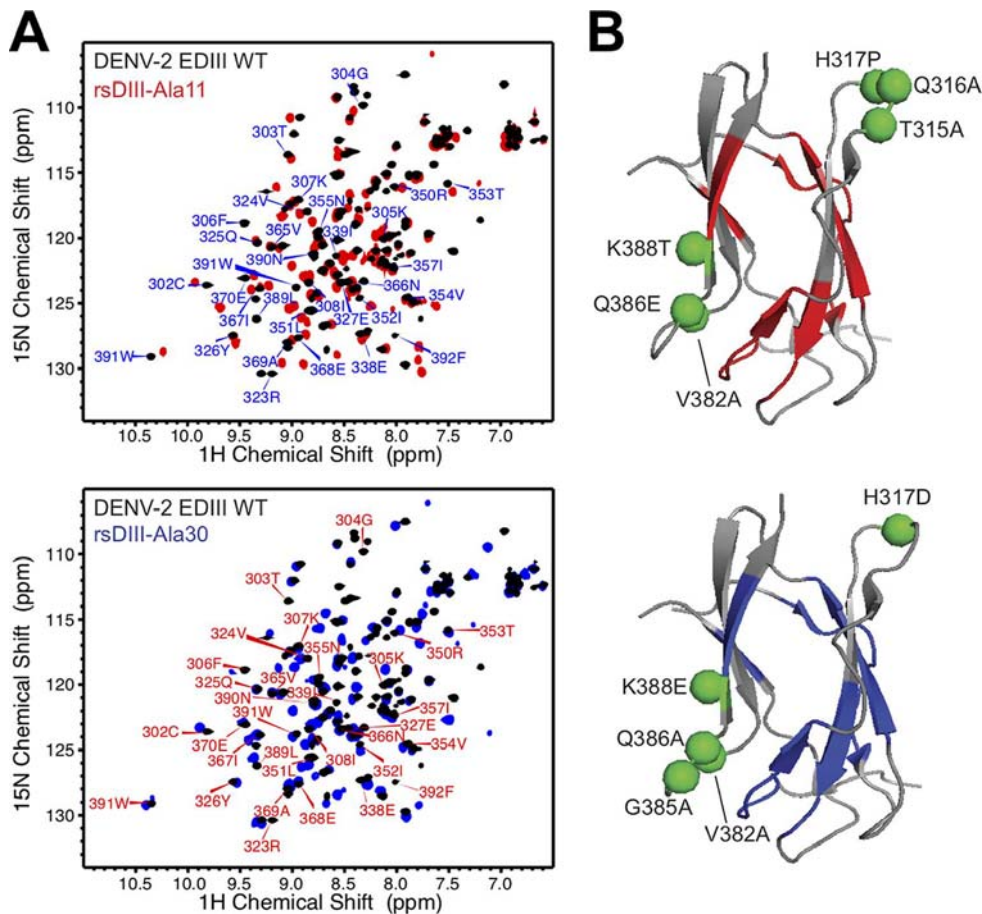


FIG 3 The core structure of rsDIIIs relative to WT DENV-2 EDIII is maintained. (A) ^1H - ^{15}N HSQC cross peaks for WT DENV-2 EDIII (black), rsDIII-Ala11 (red), and rsDIII-Ala30 (blue) overlap substantially. Residue labels for WT DENV-2 EDIII peaks that had nearby peaks in the rsDIII-Ala11 or rsDIII-Ala30 spectra are shown. Many cross peaks overlap between the spectra, indicating that the overall fold is similar between WT and rsDIII proteins. (B) RsDIII-Ala11 (red) and rsDIII-Ala30 (blue) residues that overlap assigned WT DENV-2 EDIII resonances were mapped onto the DENV-2 EDIII crystal structure (PDB ID 3UZV [27]). The green spheres represent points of mutation in rsDIIIs relative to the WT.

immunized mice demonstrated similar neutralization breadths for DENV-1 to -3, with IC_{50} titers of 1:150, 1:53, and 1:150, respectively. Sera from mice immunized with rsDIII-Ala11 were weakly neutralizing, with partial reduction of infection observed only at the highest serum concentration tested. Individual focus reduction neutralization titers (FRNT_{50} and FRNT_{80}) for sera from each mouse against DENV-1 to -3 were plotted as reciprocal titers and compared. Although FRNT_{50} and FRNT_{80} values from WT DENV-2 EDIII-immunized mice were statistically different from those from rsDIII-Ala11-immunized mice, no significant differences were observed between sera from mice immunized with WT DENV-2 EDIII and those from mice immunized with rsDIII-Ala30 (Fig. 5B).

Sera from rsDIII-Ala30- and WT DENV-2 EDIII-immunized mice are not protective in a passive-transfer model of DENV-2 infection. To test if the antibodies elicited by EDIII and rsDIIIs conferred protection against DENV-2 challenge, a stringent passive transfer of sera model of infection was employed. Sera from days 60 and 90 from the WT DENV-2 EDIII and rsDIII-Ala30 groups were pooled and transferred to groups of five AG129 mice (200- μl dose), which lack interferon alpha/beta/gamma ($\text{IFN-}\alpha/\beta/\gamma$) receptors and are vulnerable to DENV infection (69). Pooled naive serum samples were used as a negative control. Post-serum transfer, all the AG129 mice were inoculated with the mouse-adapted D2S20 DENV-2 strain (5×10^4 PFU), which has an EDIII amino acid sequence identical to that of DENV-2 16681 and which was neutralized similarly by the

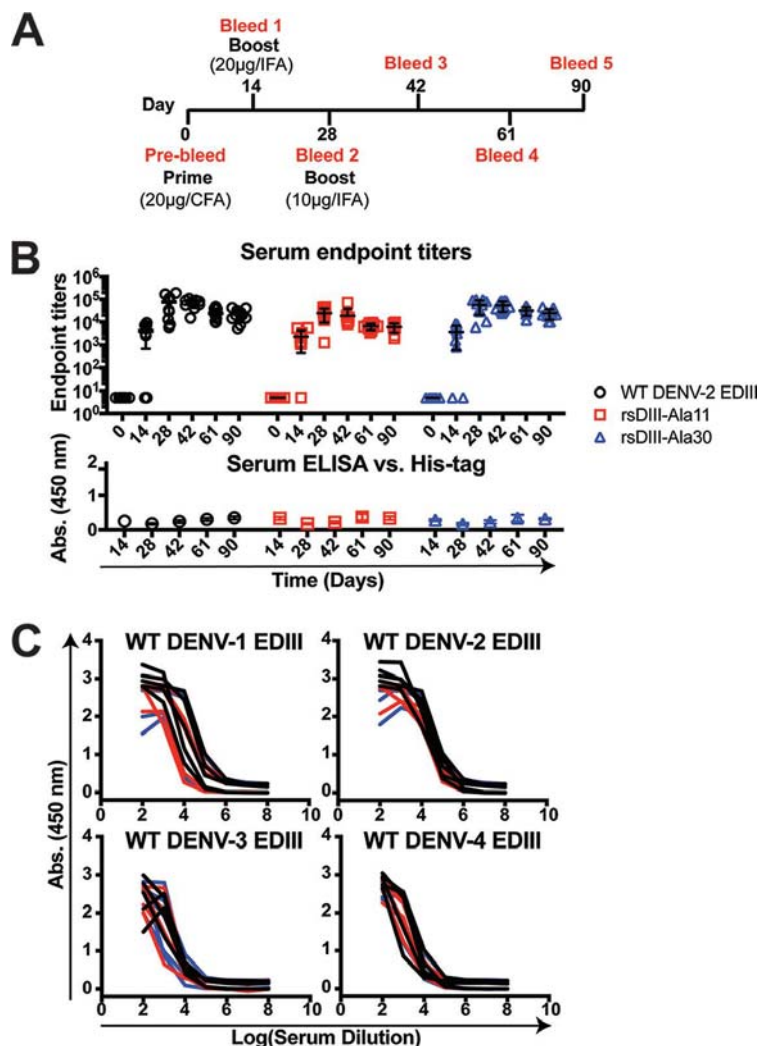


FIG 4 RsDIIIs elicit broadly reactive serum responses across DENV serotypes 1 to 4. (A) Immunization and bleed schedule. (B) (Top) Serum endpoint titers against each immunogen reached a maximum by day 28 and remained constant through day 90. (Bottom) Serum antibody responses were not directed toward a hexahistidine tag-bearing control protein. Groups of 10 BALB/c mice were immunized, and serum reactivity was determined for each mouse and plotted as the mean \pm SD. (C) ELISA against EDIIIs, with five representative serum samples from each immunogen group. The data are from a single experiment completed in duplicate.

WT DENV-2 EDIII and rsDIII-Ala 30 antisera (data not shown). All the mice that received sera from either the WT DENV-2 EDIII- or rsDIII-Ala30-immunized mice died by day 5 postinfection, whereas the mean survival time of mice receiving naive serum was 7 days (Fig. 6A). There was a statistically significant trend ($P = 0.006$) toward shortened survival time in the EDIII immunogen-treated groups relative to mice receiving naive serum, suggesting that the immunogen-elicited serum antibodies were insufficient for protection and instead resulted in ADE. Indeed, the pooled day 60/90 sera from mice receiving WT DENV-2 EDIII or rsDIII-Ala30 were shown to enhance infection relative to naive sera in K562 cells (Fig. 6B).

DISCUSSION

We describe a structure-based approach for design of resurfaced EDIII immunogens. Our mutational strategy emphasized replacement of side chains in undesirable epitopes with small side chains (Ala or Ser). This procedure resulted in rsDIIIs that maintained the broadly neutralizing A/G strand epitope but were altered in the AB loop

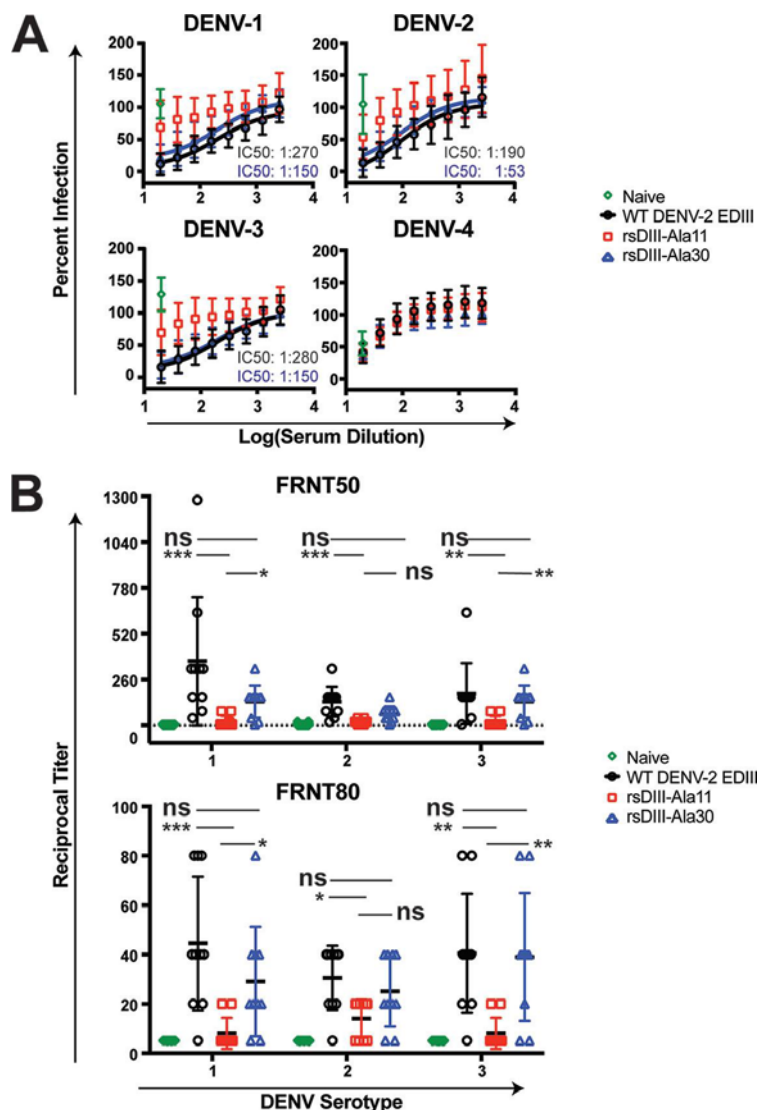


FIG 5 Engineered EDIIIs elicit potent cross-neutralizing antibodies. (A) Aggregate serum neutralization data for 10 mice against DENV-1 to -4. The lowest serum dilution tested for each sample was 1:20, followed by serial 2-fold dilutions. Naive mice served as the negative control. For DENV-1 to -3, sera from WT DENV-2 EDIII- and rsDIII-Ala30-immunized mice showed similar levels of neutralization, with the IC₅₀s indicated as serum titers. Sera from rsDIII-Ala11-immunized mice demonstrated weak neutralization. Naive sera resulted in partial neutralization at the lowest dilution tested. The data are from two experiments performed in duplicate and are plotted as means \pm SD. (B) Neutralization curves for individual mice against DENV-1 to -3 were plotted, and both 50% and 80% focus reduction neutralization titers were determined and plotted. The mean FRNT₅₀ and FRNT₈₀ values for WT DENV-2 EDIII-immunized and rsDIII-Ala30-immunized mice were not significantly different (ns), whereas the mean FRNT₅₀ and FRNT₈₀ values for WT DENV-2 EDIII- and rsDIII-Ala11-immunized mice were significantly different by Kruskal-Wallis one-way ANOVA with Dunn's multiple-comparison test (*, $P < 0.05$; **, $P < 0.01$; ***, $P < 0.001$). For serum samples that did not reach 50% or 80% neutralization at the highest concentration of serum tested (1:20 dilution), a serum dilution of 1:5 was arbitrarily assigned.

(targeted by cross-reactive, nonneutralizing antibodies) and FG loops (targeted by serotype-specific antibodies).

In vitro characterization of rsDIIIs and WT DENV-2 EDIII indicated that resurfacing mutations did not alter the conformational integrity of the broadly neutralizing A/G strand epitope, as evidenced by binding of rsDIIIs to 4E11, but provided remodeled AB and FG loops that could no longer be recognized with high affinity by prototypic MAb targeting the region (2H12 and 3H5). Furthermore, ¹⁵N-¹H HSQC spectra from WT DENV-2 EDIII, rsDIII-Ala11, and rsDIII-Ala30 had substantial cross-peak overlap, especially at resonances that corresponded to the EDIII core. Since HSQC nuclear magnetic

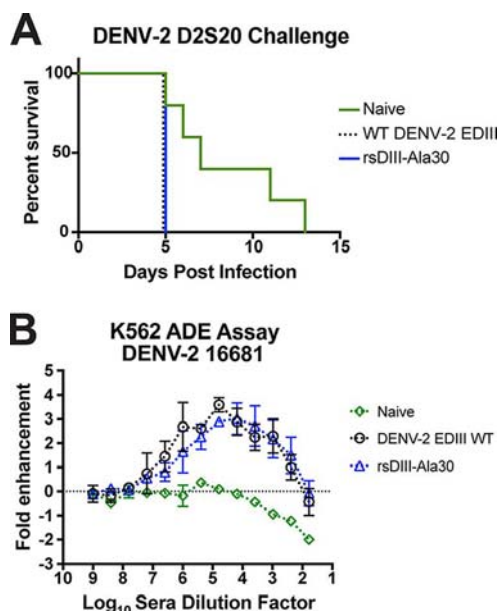


FIG 6 AG129 passive-transfer model of DENV-2 D2S20 infection, and ADE assay. (A) Pooled sera from days 60 and 90 from WT DENV-2 EDIII- and rsDIII-Ala30-immunized mice were transferred to groups of 5 AG129 mice prior to infection with the mouse-adapted strain D2S20 of DENV-2. Pooled naive sera served as the negative control. The mice were monitored until death. All the mice from the WT- and rsDIII-Ala30-immunized groups died on day 5, while naive mice had a mean survival of 7 days. By log rank test, there was a statistically significant trend ($P = 0.006$) toward shortened survival in the EDIII immunogen-treated groups relative to mice receiving naive serum, suggesting that the immunogen-elicited serum antibodies were insufficient for protection and instead resulted in ADE. The data are from a single experiment. (B) DENV-2 16681 RVPs were incubated with serial dilutions of the indicated mouse sera for 1 h at 37°C, followed by infection of K562 cells. Infection was measured by flow cytometry 48 h later. The fold enhancement was calculated in reference to the minimal infection of K562 cells in the absence of antibody. Shown is one representative experiment of two; the error bars indicate the ranges of duplicate technical replicates.

resonance (NMR) signals depend on the local microenvironment, these results indicate that mutations within the AB and FG loops did not alter the core EDIII fold. Furthermore, many of the chemical shifts in the rsDIII spectra that closely overlapped peaks in the WT DENV-2 EDIII spectrum could be traced back to the A and G strands, further indicating that the bNAb epitope was maintained in rsDIIIs.

The resurfacing mutations in rsDIII-Ala11 and rsDIII-Ala30 did not compromise the ability of rsDIIIs to induce immunogen-specific antibody titers in comparison to WT DENV-2 EDIII. The overall serum antibody endpoint titers of each immunogen group were similar, suggesting that rsDIIIs were efficiently presented to immune cells. Furthermore, each immunogen elicited sera that were broadly reactive with EDIIIs from all four serotypes. Overall binding to all four EDIIIs was similar for sera from each immunogen, indicating elicitation of antibodies to cross-reactive epitopes, whether from the A/G strand, AB loop, or other conserved regions.

Both WT DENV-2 EDIII and rsDIII-Ala30 elicited sera that were cross-neutralizing for DENV-1 to -3, with IC_{50} s of $>1:100$ in most cases. In comparison, previous immunogenicity studies with WT DENV-2 EDIII demonstrated neutralization of only the homologous virus, with only very weak cross-neutralization of heterologous virus (35, 36, 41, 42, 58). Thus, results with sera elicited from our preparation of WT DENV-2 EDIII were unanticipated. The differences in our WT DENV-2 EDIII construct could be due, in part, to our choice of domain boundaries for EDIII, which were based upon X-ray crystallography structures (27). We defined the domain boundary to include only residues of EDIII, whereas some of the prior EDIII constructs contained regions of EDI that could potentially skew the immune response (38, 70). Additional residues added to the N or C terminus of EDIII could alter antigen processing and thus presentation of epitopes to immune cells (71). Another contributing factor could be the extent of aggregate EDIII

present in the preparation used for immunization. Our study utilized exclusively monomeric EDIII, purified by SEC, which could potentially enrich the antibody response toward discontinuous, conformational epitopes, such as the A/G strand, relative to preparations containing significant proportions of aggregated EDIII that might emphasize linear epitopes, such as the AB or FG loop. Finally, differences in adjuvants, immunization schemes, and the genetic backgrounds of mice can also influence the antibody repertoire.

Although rsDIII-Ala11 and rsDIII-Ala30 differ by only 6 residues, display similar biochemical properties, and elicited similar antibody endpoint titers in mice, they induced distinct neutralization profiles. Sera from the rsDIII-Ala11-immunized group barely reached 50% reduction of infection at the highest serum concentration tested for all three serotypes, whereas sera from both WT DENV-2 EDIII- and rsDIII-Ala30-immunized groups neutralized greater than 90% of virus infection at this dilution. The cause of this difference in elicited antibodies is unknown, given that the sequences of all three immunogens are highly similar. However, rsDIII-Ala11 contained three substitutions in the AB loop relative to WT DENV-2 EDIII, whereas rsDIII-Ala30 contained only one. It is possible that significant mutation of the AB loop alters the processing and antigen presentation of EDIII-based immunogens, which results in fewer neutralizing antibodies.

Analysis of neutralization titers for the WT DENV-2 EDIII group demonstrated that all the mice mounted inhibitory antibody responses against all three serotypes, and in particular, one mouse showed greater neutralization, with EC_{50} s of 1:1280, 1:320, and 1:640 for DENV-1, DENV-2, and DENV-3, respectively. As was seen with the rsDIII-Ala30-immunized group, and for unexplained reasons, the WT DENV-2 EDIII-immunized group also developed lower neutralization titers against homologous virus. The WT DENV-2 EDIII and rsDIII-Ala30 groups demonstrated similar $FRNT_{50}$ and $FRNT_{80}$ values. Therefore, rsDIII-Ala30 has favorable immunogenic properties, as it elicited cross-neutralizing antibodies but does not contain a critical AB loop residue, H317. Whether this alteration in the AB loop leads to a lower proportion of nonneutralizing AB loop antibodies remains to be determined.

Although sera from both WT- and rsDIII-immunized mice elicited cross-neutralizing responses, they did not protect in a stringent AG129 passive-transfer model of DENV-2 infection with a dose of 200 μ l ($FRNT_{50}$ \sim 1:60 to 1:120) per mouse. Rather, enhancement of infection was evident, as mice receiving naive sera showed prolonged survival relative to the mice that received either the WT DENV-2 EDIII or rsDIII-Ala30 immunogen-elicited sera and as demonstrated *in vitro* in K562 cells. Similar disease enhancement was reported in AG129 mice treated with homologous anti-DENV-2 sera at doses of <100 μ l per mouse ($FRNT_{50}$ \sim 1:67), with all the mice succumbing by day 4 upon challenge with DENV-2 D2S10 (72). However, full protection was observed with a dose of 400 μ l per mouse ($FRNT_{50}$ \sim 1:412). In another study, only 50% of mice receiving 200 μ l each of homologous high-titer ($FRNT_{50}$, 10^3 to 10^4 dilution) anti-DENV-2 serum on days -1 and $+1$ of infection survived challenge with 10^4 PFU of DENV-2 S221, and it was noted that serum containing higher neutralizing titers demonstrated full protection (73). Thus, our results are consistent with previous studies and suggest that larger amounts of sera, or induction of a more potent neutralization response, is required for protection in AG129 mice.

The protection results presented here contrast with previous EDIII immunogenicity reports, which have demonstrated varying degrees of protection against homologous virus using an intracranial challenge (IC) of BALB/c immunocompetent mice (36, 40, 74, 75). The AG129 passive-transfer model is a potentially more stringent model of DENV infection, as these mice are immunocompromised and lack type I and II IFN responses; indeed, in some cases, intracranial challenge with DENV does not induce mortality (70). Based on titers achieved with natural infection (72), we hypothesize that cross-neutralizing titers higher than those observed here will be required to see protection against DENV challenge. To that end, multivalent presentation strategies, in which multiple copies of EDIII or rsDIIIs are presented on a nanoparticle to boost immunogenicity, provide a possible route for induc-

ing protective cross-neutralizing responses with rsDIII-Ala30. Additionally, prime-boost strategies with live-attenuated viruses and rsDIIIs can be evaluated to determine whether resurfaced EDIIIs can boost and broaden immunity to DENV.

The approach for EDIII resurfacing complements previously reported approaches to broadening the EDIII antibody response. Several groups have explored mixtures of EDIIIs and fusion of all four EDIIIs ("beads on a string"), as well as a consensus sequence EDIII, as immunogens (58, 76, 77). Murine antibody responses to EDIII cocktails were unbalanced, favoring neutralization of DENV-1 and DENV-2 over DENV-3 and DENV-4 (58). The fusion protein consisting of all four EDIIIs elicited unbalanced neutralizing responses across the four serotypes, most potently inhibiting DENV-4 (FRNT₅₀, 1:479 in Freund's adjuvant) and least potently inhibiting DENV-2 (1:118 in Freund's adjuvant) (76). Finally, the consensus EDIII produced weakly neutralizing antibody responses against all four serotypes (77). In this study, we used Freund's adjuvant to allow direct comparison to previous reports using similar immunization strategies. Other EDIII immunization studies using aluminum-containing adjuvants or Montanide ISA 720 yielded similar overall neutralizing titers in mice (generally, FRNT₅₀ values of <1:500) (35, 38, 42, 76). One potential advantage of the WT DENV-2 EDIII and rsDIII-Ala30 immunogens described here is that they induce cross-reactive (DENV-1 to -4) responses that are partially cross-neutralizing (DENV-1 to -3) in comparison to the single-component EDIII-based constructs that have been described previously (35, 38, 42, 76), albeit without substantial improvement in homotypic neutralizing titers. In addition to the multivalent presentation strategies discussed above, exploration of alternate adjuvants to boost the neutralizing response is warranted.

In summary, our data support the feasibility of epitope focusing and resurfacing by mutation as an immunogen design strategy for DENV EDIII. Future work to map the epitopes targeted by monoclonal antibodies elicited from rsDIII immunization could direct next-generation EDIII design. In light of the immune cross talk among flaviviruses, and in particular between DENV and ZIKV (78–82), similar approaches could be extended to ZIKV EDIII and other emerging flaviviruses of global concern (83).

MATERIALS AND METHODS

Animals. Female BALB/c mice were purchased from Charles River Laboratories and housed in ventilated cages with access to unlimited food, water, and bedding. Female AG129 mice, which lack IFN- $\alpha/\beta/\gamma$ and are thus susceptible to DENV infection, were bred at Washington University and housed in ventilated cages with access to unlimited food, water, and bedding for challenge experiments. Experiments were carried out in accordance with the recommendations in the Guide for the Care and Use of Laboratory Animals of the National Institutes of Health after approval by the Institutional Animal Care and Use Committees at the Albert Einstein College of Medicine and the Washington University School of Medicine.

Cell lines. African green monkey kidney Vero cells (World Health Organization [WHO]) (ECACC 88020401) cells (Research Resource Identifier [RRID] CVCL_JF53) were cultured in Dulbecco's modified Eagle medium (DMEM) supplemented with 10% fetal bovine serum (FBS), 1% penicillin-streptomycin (P/S), and 1 \times L-glutamine at 37°C and 5% CO₂. C6/36 *A. albopictus* mosquito cells (ATCC; RRID CVCL_Z230) were maintained in DMEM containing 10% FBS, 1% penicillin-streptomycin, 1 \times L-glutamine, 2 \times nonessential amino acids, and 1 \times HEPEs at 28°C and 5% CO₂. FreeStyle 293-F cells (Thermo Fisher Scientific, Waltham, MA; RRID CVCL_D603), suspension cells derived from HEK293 (human embryonic kidney) cells, were cultured in FreeStyle 293 expression medium supplemented with 1% penicillin-streptomycin at 37°C, 8% CO₂, and 120 rpm. The 4E11 (ATCC; RRID CVCL_J730) and 2H12 hybridoma cell lines were provided by F. Arenzana-Seisdedos (Institut Pasteur, Paris, France) and Gavin Screaton (Imperial College London, London, United Kingdom), respectively. 3H5 hybridoma cells were purchased from the ATCC (RRID CVCL_D292). All hybridoma cell lines were cultured in RPMI-1650 medium supplemented with 15% fetal calf serum (FCS), 2% L-glutamine, 1% sodium pyruvate, 1% penicillin-streptomycin, 0.2% gentamicin, and 0.1% 2-mercaptoethanol at 37°C and 8% CO₂.

Viruses. The DENV strains used in neutralization assays were as follows: DENV-1, 16007; DENV-2, 16681; DENV-3, 16652; and DENV-4, 1036 (World Arbovirus Reference Center, University of Texas Medical Branch [UTMB], Galveston, TX). Briefly, confluent C6/36 (mosquito) cells were infected at a multiplicity of infection (MOI) of 0.05 to 0.01 with DENV and incubated for approximately 5 days at 28°C and 5% CO₂ or until cytopathic effects were apparent. Virus-containing cell supernatants were harvested by ultracentrifugation and pelleted through a 25% (vol/vol) glycerol in TNE (50 mM Tris-HCl, pH 7.4, 100 mM NaCl, 0.1 mM EDTA) cushion (84).

Antibody purification. 4E11, 4E5A, and 2H12 (IgG2a, IgG2a, and IgG2b, respectively) were purified with protein A affinity agarose beads and the Gentle Antibody Elution system (Pierce, ThermoScientific, Rockford, IL) according to the manufacturer's protocol. 3H5 (IgG1) was purified using protein G affinity agarose beads and a protein G binding buffer system (Pierce, ThermoScientific, Rockford, IL) following

the manufacturer's protocol. All the antibodies were desalted in 150 mM HEPES, pH 7.4, 200 mM NaCl and analyzed by sodium dodecyl sulfate-polyacrylamide gel electrophoresis (SDS-PAGE) to determine purity. Purified WNV-E111 antibody was described previously (31).

Phage display of DENV-2 EDIII. The display of wild-type DENV-2 EDIII (strain Jamaica/1409/1983) was previously described (59). EDIII-expressing phage particles were produced by electroporation into *Escherichia coli* XL1-Blue cells (Agilent Technologies, Santa Clara, CA) and recovered in 2× yeast extract tryptone (YT) medium containing 50 µg/ml carbenicillin and 10 µg/ml tetracycline at 37°C and 220 rpm for 5 h. Phage were coinfecting with M13KO7 helper phage (New England BioLabs, Ipswich, MA) at a final concentration of 10¹⁰ PFU per ml and incubated for 1 h at 37°C and 220 rpm. A final concentration of 50 µg/ml kanamycin was added, and the culture was incubated overnight at 37°C and 220 rpm. Phage were harvested by precipitation with 4% (wt/vol) polyethylene glycol (PEG) 8000 and 3% (wt/vol) NaCl after centrifugation to remove cells. The precipitated phage were centrifuged at 17,000 × g for 20 min at 4°C and resuspended in 1 ml PB-T (phosphate-buffered saline [PBS] containing 0.5% [wt/vol] BSA and 0.05% [vol/vol] Tween 20).

Surface expression of EDIII was confirmed by phage ELISA against the anti-FLAG monoclonal antibody M2. Folding of EDIII was confirmed by phage ELISA against 4E11, a conformation-sensitive antibody. For phage ELISA, antibodies were immobilized on Costar EIA/RIA high-binding plates at 0.5 µg per well in PBS, pH 8.0, overnight at 4°C; wells coated with 1% (wt/vol) BSA served as negative controls. The wells were blocked with PBS containing 1% (wt/vol) BSA for 2 h at room temperature (RT). Phage were serially diluted 1:10 in PB-T, added to the wells, and incubated for 1 h at RT. The wells were washed extensively with PBS-T (PBS containing 0.05% [vol/vol] Tween 20), followed by the addition of a horseradish peroxidase (HRP)-conjugated anti-M13 monoclonal antibody diluted 1:1,000 in PB-T for 1 h at RT. The wells were washed as before. The ELISA was developed by the addition of substrate, 3,3',5,5'-tetramethylbenzidine (TMB), and quenched with 0.5 M sulfuric acid. The absorbance read at 450 nm served as a readout for binding.

Resurfacing phage display library design and construction. An inactive template DNA for DENV-2 EDIII was produced in which positions to be varied in the library were mutated to stop codons (TAA). The libraries were produced using Kunkel mutagenesis, as previously described (59, 66). Each reaction mixture contained 10 µg of template uracil-enriched single-stranded DNA (dU-ssDNA) and a 3-fold excess of 5'-phosphorylated library primers that encoded the designed degeneracy. Library DNA was purified and electroporated into *E. coli* SS320 cells (Lucigen, Madison, WI) to yield 2.5 × 10⁹ and 1 × 10⁹ transformants for the serine and alanine libraries, respectively. The theoretical diversities for the serine and alanine libraries were 1.7 × 10⁷ and 5.2 × 10⁵, respectively. Thus, the library size exceeded both theoretical diversities by at least 100-fold, indicating that sampling of the full sequence space was sufficient.

Phage library selection and screening. To isolate EDIII mutants that maintained high affinity for the bNAb 4E11, both resurfacing libraries were subjected to three rounds of selection at increasing stringency against 4E11 prior to screening. For each selection, wells were coated with 0.5 µg per well of 4E11. Phage were added and incubated for 1 h at RT. Unbound phage were removed by washing with PBS-T. Bound phage were eluted with 100 mM glycine, pH 2.0, into 2 M Tris buffer, pH 7.5. The output population was amplified by infecting *E. coli* XL1-Blue cells, coinfecting with M13KO7 helper phage, and precipitating as described above. A well containing 1% (wt/vol) BSA served as the negative control in each round of selection in order to monitor background enrichment of 4E11-specific phage.

Individual phage clones were screened for binding to 4E11 using a monoclonal phage ELISA. Individual phage clones were grown in 1 ml 2× YT medium supplemented with 100 µg/ml carbenicillin and 10¹⁰ PFU per ml helper phage in a 96-deep-well plate. Cells were pelleted by centrifugation, and phage-containing supernatants were applied to 96-well plates containing 4E11 (0.5 µg per well), 1% (wt/vol) BSA (negative control), or M2 antibody at a 1:500 dilution (expression control). The rest of the ELISA was performed as described for the phage ELISA above. The absorbance at 450 nm served as a readout for binding, and the absorbance values for binding to 4E11 were compared to the BSA absorbance values. Clones from both the alanine and serine libraries that demonstrated a >2-fold preference for binding to 4E11 over the negative control were selected for further characterization by phage ELISA against 4E11, 4E5A, 2H12, WNV-E111, and 3H5 antibodies.

Expression and purification of soluble rDIII. WT DENV-2 EDIII and rDIII were cloned into a pSGC vector based on the pET28a plasmid, using ligation-independent cloning (LIC). Constructs were expressed with an N-terminal hexahistidine tag, followed by a tobacco etch virus (TEV) protease cleavage site. EDIII were transformed into T7 Express competent *E. coli* cells (New England BioLabs, Ipswich, MA) and incubated on Luria-Bertani (LB)/kanamycin agar plates overnight at 37°C. A 25-ml starter culture from a single colony in 2× YT medium was incubated overnight at 37°C and 220 rpm. The starter culture was used to inoculate 2 liters of 2× YT medium in a LEX 48 airlift fermentor and incubated for 3 h at 37°C to an optical density at 600 nm (OD₆₀₀) of approximately 0.8. Cultures were induced with a final concentration of 1 mM isopropyl-β-D-1-thiogalactopyranoside (IPTG) and incubated at 22°C overnight. Cells were harvested by centrifugation and stored at -80°C until purification.

Cells were lysed by sonication in lysis buffer [50 mM Tris-HCl, pH 7.5, 500 mM NaCl, 5 mM imidazole, 1 mM tris(2-carboxyethyl)phosphine (TCEP), and 6 M urea] to solubilize inclusion bodies. The lysate was clarified by centrifugation, and the supernatant was applied to a Ni-NTA affinity resin (Qiagen, Hilden, Germany) that was preequilibrated with lysis buffer. The column was washed with 3 column volumes (CV) of buffer A (lysis buffer containing 10 mM imidazole), 4 CV of buffer B (lysis buffer containing 20 mM imidazole), and 4 CV of buffer C (lysis buffer containing 30 mM imidazole). EDIII were eluted with 1.5 CV of elution buffer (lysis buffer containing 250 mM imidazole). Fractions were pooled based on SDS-PAGE

TABLE 1 Apparent dissociation constants for rsDIIIs

Antibody	Parameter	Value		
		WT DENV-2 EDIII	rsDIII-Ala11	rsDIII-Ala30
4E11	k_d/k_a (nM)	0.01 ± 0.002	0.45 ± 0.11	0.03 ± 0.001
	k_a ($M^{-1} s^{-1}$)	$(1.4 \pm 0.008) \times 10^6$	$(27 \pm 1.2) \times 10^4$	$(220 \pm 1.6) \times 10^4$
	k_d (s^{-1})	$(19 \pm 2.2) \times 10^{-6}$	$(120 \pm 3.9) \times 10^{-6}$	$(54 \pm 2.6) \times 10^{-6}$
2H12	k_d/k_a (nM)	1.1 ± 19		
	k_a ($M^{-1} s^{-1}$)	$(1.8 \pm 3.3) \times 10^6$		
	k_d (s^{-1})	$(92 \pm 2.1) \times 10^{-5}$		
3H5	k_d/k_a (nM)	120 ± 0.32		
	k_a ($M^{-1} s^{-1}$)	$(1.4 \pm 1.4) \times 10^3$		
	k_d (s^{-1})	$(1.6 \pm 0.04) \times 10^{-4}$		

analysis. Denatured EDIIIs were refolded by fast dilution (1:100 dilution added dropwise) into refolding buffer (20 mM HEPES, pH 7.5, 100 mM NaCl, 400 mM L-arginine, and 5% [vol/vol] glycerol) and incubated overnight at 4°C. Refolded EDIIIs were centrifuged to remove aggregated protein and concentrated using a 3,000 molecular weight cutoff (MWCO) Amicon (Millipore, Billerica, MA). Concentrated EDIIIs were dialyzed against refolding buffer at 4°C for 4 h. Three rounds of dialysis were performed. The EDIIIs were then filtered through a 0.2- μ m filter and applied to a HiLoad Superdex 200 16/600 preparatory-grade (pg) column (GE Healthcare, Little Chalfont, United Kingdom) using refolding buffer as the running buffer. The monomeric fractions were pooled and concentrated to final concentrations ranging from 0.5 to 1.1 mg/ml. Proteins were stored at 4°C until use.

Soluble rsDIII biochemical characterization. The binding profiles for WT DENV-2 EDIII and rsDIIIs were determined by ELISA. Coming enzyme immunoassay (EIA) half-area well plates (Coming, Corning, NY) were coated with 0.2 μ g per well of rsDIII in PBS, pH 8.0, overnight at 4°C; 1% (wt/vol) BSA-coated wells served as the negative control. The wells were blocked with 1% (wt/vol) BSA in PBS for 2 h at RT. Purified antibodies (4E11, 2H12, and 3H5) were diluted 1:1 starting at 20 μ g/ml (approximately 133 nM) in PB-T and incubated with immobilized rsDIII for 1 h at RT. The wells were extensively washed with PBS-T, and a 1:1,000 dilution of protein A-HRP (Invitrogen, Carlsbad, CA) was added for 1 h at RT. The plates were washed with PBS-T, developed using TMB, and quenched with 0.5 M sulfuric acid. The absorbance was read at 450 nm. The data were fit to a standard three-parameter logistic equation using GraphPad Prism (GraphPad Software, La Jolla, CA). The EC_{50} s were determined from the inflection point on the curve.

To determine the rate constants for rsDIII binding to DENV antibodies (Table 1), the ForteBio BLITZ system was used. Ni-NTA sensors were used to load His-tagged rsDIII or WT DENV-2 EDIII, followed by antibody (4E11, 2H12, and 3H5) association and dissociation. Several concentrations of antibodies were used, ranging from 27 to 0.01 nM for 4E11 and 2H12 and from 6 to 0.01 μ M for 3H5. To estimate the k_a (association rate constant), and k_d (dissociation rate constant), a global 1:1 binding model was used.

rsDIII HSQC NMR. To compare the fold of rsDIIIs with WT DENV-2 EDIII, ^{15}N - ^{13}C double-labeled proteins were produced using the method of Marley et al., and 3D NMR experiments were conducted (85). Briefly, rsDIII-Ala11, rsDIII-Ala30, and WT DENV-2 EDIII constructs were transformed into T7 Express competent cells as before. A starter culture of 25 ml 2 \times YT medium containing 50 μ g/ml kanamycin was grown overnight at 37°C at 220 rpm. The starter culture was transferred to 2 liter 2 \times YT medium containing 50 μ g/ml kanamycin and grown at 37°C and 220 rpm until the cell density reached an OD_{600} of approximately 1.0. Cells were harvested by centrifugation and rinsed briefly with M9 minimal medium (per liter, 6.5 g sodium phosphate dibasic, 3 g potassium phosphate monobasic, 0.5 g NaCl) completed with 1 \times minimal essential medium (MEM) vitamin solution (Thermo Fisher Scientific, Waltham, MA), trace elements, and 1 mM $MgSO_4$. Cell pellets were resuspended in 1 liter of completed M9 minimal medium containing 2 g ^{15}N -labeled ammonium chloride for rsDIII-Ala11 and rsDIII-Ala30, and both labeled ammonium chloride and 3 g ^{13}C -labeled D-glucose for WT DENV-2 EDIII (Cambridge Isotope Laboratories, Inc., Andover, MA). Cultures were incubated for 1 h at 37°C and 220 rpm. Expression was induced by adding 1 mM IPTG and incubating at 22°C at 220 rpm overnight. Cells were harvested by centrifugation and stored at -80°C. Double-labeled WT DENV-2 EDIII and ^{15}N -labeled rsDIIIs were purified as described above. Prior to performing experiments, rsDIIIs were buffer exchanged into 20 mM sodium phosphate, pH 7.5, and 50 mM NaCl and concentrated to final concentrations of 78 μ M (rsDIII-Ala11) and 390 μ M (rsDIII-Ala30). Double-labeled WT DENV-2 EDIII was buffer exchanged into 20 mM sodium phosphate, pH 6.5, 50 mM NaCl, and 50 mM L-arginine and concentrated to a final concentration of 164 μ M.

All NMR experiments were collected at 25°C on 600 MHz cryoprobe-equipped Bruker or Varian instruments. HSQC-based pulse sequences were used for WT DENV-2 EDIII, rsDIII-Ala11, and rsDIII-Ala30. Chemical-shift assignments were made for the core of the WT DENV-2 EDIII protein using three-dimensional HNCO, HNCA, HNCoCA, HNCaCO, HNCACB, and HNCoCACB triple-resonance data sets. All 3D experiments were recorded with nonuniform sampling and processed with MddNMR (86) and NMRPipe (87). Backbone resonance assignments and comparisons of wild-type and mutant EDIII spectra were made using CCPN Analysis (88). Chemical shift referencing was made with respect to 4,4-dimethyl-4-silapentane-1-sulfonic acid (DSS-2).

Mouse immunizations. Groups of 10 6-week-old female BALB/c mice were immunized i.p. with 20 μ g of either WT DENV-2 EDIII, rsDIII-Ala11, or rsDIII-Ala30 in CFA on day 0. Prior to immunization,

all the mice were bled by tail vein nick, and this naive serum served as the negative control for all further experiments. The mice were subsequently immunized on days 14 and 28 with 20 μ g and 10 μ g of proteins, respectively, in IFA. The mice were bled on days 14, 28, 45, 60, and 90. Serum was harvested using a serum separator tube (Sarstedt AG & Co.) by centrifugation at $6,000 \times g$ for 2.5 min at 4°C. All serum samples were stored at -20°C until use. Prior to neutralization assays, serum samples were heat inactivated by incubating at 56°C for 15 min, followed by microcentrifugation at $13,000 \times g$ for 5 min. The serum was subsequently transferred to a clean microcentrifuge tube, avoiding any pelleted material.

Serum ELISAs. Endpoint serum antibody titers were measured by ELISA against the respective EDIII and calculated as described below. In brief, Corning EIA half-area well plates were coated with WT or mutant EDIIIs at 0.2 μ g per well overnight at 4°C in PBS, pH 8.0. Serum samples collected at each time point were serially diluted (1:10) starting at a 1:100 dilution in PB-T. The serum was incubated for 1 h at RT prior to extensive washing with PBS-T. A 1:10,000 dilution of anti-mouse-HRP antibody (Jackson ImmunoResearch Laboratories, Inc., West Grove, PA) was added and allowed to incubate for 1 h at RT. Following extensive washing, the plates were developed by the addition of TMB and quenched with 0.5 M sulfuric acid. Endpoint titers were determined for each serum sample at days 14, 28, 45, 60, and 90 by subtracting the naive serum absorbance values, fitting them to a four-parameter logistics curve, and determining the EC_{50} for each mouse.

Serum neutralization assays. To determine the neutralization potency and breadth of each serum sample, FRNTs using Vero cells were completed for serum samples collected on days 0 (naive serum; negative control), 60, and 90, as detailed previously (89). The data were fit to standard three-parameter logistic equations in GraphPad Prism (GraphPad Software, La Jolla, CA), and the IC_{50} s were determined from the inflection points of the curves.

AG129 passive-transfer model of DENV-2 infection. Sera from WT DENV-2 EDIII- and rsDIII-Ala30-immunized mice from days 60 and 90 or naive mice (day 0) were pooled separately and tested in neutralization assays to determine the pooled FRNT_{50} for DENV-2 (FRNT_{50} values of 1:640 and 1:320 for WT DENV-2 EDIII and rsDIII-Ala30 pooled sera, respectively). Two hundred microliters of sera from each immunogen group were transferred (i.p.) to groups of 5 AG129 mice (Marshall BioResources, North Rose, NY) on day -1 . All AG129 mice were inoculated intravenously (i.v.) with 5×10^4 PFU of mouse-adapted DENV-2 strain D2S20 on day 0. The mice were monitored for morbidity and mortality for 13 days.

Statistical analyses. All statistical analyses were performed with GraphPad Prism software. *P* values of <0.05 were considered statistically significant. Serum FRNT_{50} and FRNT_{80} values were compared by Kruskal-Wallis one-way analysis of variance (ANOVA) with Dunn's multiple-comparison correction. For survival studies, the log rank test was used to compare groups.

Antibody-dependent enhancement assay. Reporter virus particles (RVPs) incorporating the structural proteins of DENV-2 strain 16681 were produced by complementation of a subgenomic green fluorescent protein (GFP)-expressing replicon derived from a lineage II strain of WNV, as previously described (90). Serial dilutions of heat-inactivated mouse sera were incubated with DENV-2 RVPs for 1 h at 37°C , followed by the addition of K562 cells that expressed the Fc- γ receptor CD32A. Two days later, infection was scored as a function of GFP expression by flow cytometry.

SUPPLEMENTAL MATERIAL

Supplemental material for this article may be found at <https://doi.org/10.1128/JVI.01023-18>.

SUPPLEMENTAL FILE 1, XLSX file, 0.1 MB.

ACKNOWLEDGMENTS

This work was funded by the National Institutes of Health (R21-AI128090 to J.R.L., P01-AI106695 to M.S.D., and R01-AI075647 to M.K.). J.C.F. was supported in part by T32-GM007491. J.R.L. gratefully acknowledges the Irma T. Hirschl/Monique Weill Caulier Career Scientist Award, which helped fund this work. T.C.P. and K.A.D. were supported by the intramural program of NIAID.

The Albert Einstein College of Medicine has filed a provisional patent application entitled "Variants of Dengue Virus Glycoprotein E DIII and Uses Thereof" with J.R.L., J.C.F., and M.K. as coinventors. M.S.D. is a consultant for Inbios, Takeda Vaccines, and Sanofi-Pasteur and is on the Scientific Advisory Board of Moderna.

REFERENCES

- Gubler DJ, Kuno G, Markoff L. 2007. Flaviviruses, p 1153–1253. *In* Knipe DM, Howley PM, Griffin DE, Lamb RA, Martin MA, Roizman B, Straus SE (ed), *Fields virology*, 5th ed. Lippincott Williams & Wilkins, Philadelphia, PA.
- WHO. 2008. Dengue haemorrhagic fever. Factsheet no. 117, revised May 2008, p 25–28. World Health Organization, Geneva, Switzerland.
- Rice C. 1996. Flaviviridae: the viruses and their replication, p 931–959. *In* Fields BN, Knipe DM, Howley PM (ed), *Fields virology*. Lippincott-Raven, Philadelphia, PA.
- Sangkawibha N, Rojanasuphot S, Ahandrik S, Viriyapongse S, Jatanasen S, Salitul V, Phanthumachinda B, Halstead SB. 1984. Risk factors in dengue shock syndrome: a prospective epidemiologic study in Rayong, Thailand. I. The 1980 outbreak. *Am J Epidemiol* 120:653–669.
- Halstead SB. 2003. Neutralization and antibody-dependent enhance-

- ment of dengue viruses. *Adv Virus Res* 60:421–467. [https://doi.org/10.1016/S0065-3527\(03\)60011-4](https://doi.org/10.1016/S0065-3527(03)60011-4).
6. Halstead S, Chow J, Marchette N. 1973. Immunological enhancement of dengue virus replication. *Nature New Biol* 243:24–25.
 7. Halstead S, O'Rourke E. 1977. Dengue viruses and mononuclear phagocytes. I. Infection enhancement by non-neutralizing antibody. *J Exp Med* 146:201–217.
 8. Halstead SB. 2016. Critique of World Health Organization recommendation of a dengue vaccine. *J Infect Dis* 214:1793–1795.
 9. WHO. 1997. Dengue haemorrhagic fever: diagnosis, treatment, prevention and control. WHO, Geneva, Switzerland. <http://www.who.int/csr/resources/publications/dengue/Denguepublication/en/>.
 10. Guy B, Briand O, Lang J, Saville M, Jackson N. 2015. Development of the Sanofi Pasteur tetravalent dengue vaccine: One more step forward. *Vaccine* 33:7100–7111. <https://doi.org/10.1016/j.vaccine.2015.09.108>.
 11. Villar L, Dayan GH, Arredondo-García JL, Rivera DM, Cunha R, Deseda C, Reynales H, Costa MS, Morales-Ramírez JO, Carrasquilla G. 2015. Efficacy of a tetravalent dengue vaccine in children in Latin America. *N Engl J Med* 372:113–123. <https://doi.org/10.1056/NEJMoa1411037>.
 12. Capeding MR, Tran NH, Hadinegoro SRS, Ismail HIHM, Chotpitayasunondh T, Chua MN, Luong CQ, Rusmil K, Wirawan DN, Nallusamy R. 2014. Clinical efficacy and safety of a novel tetravalent dengue vaccine in healthy children in Asia: a phase 3, randomised, observer-masked, placebo-controlled trial. *Lancet* 384:1358–1365. [https://doi.org/10.1016/S0140-6736\(14\)61060-6](https://doi.org/10.1016/S0140-6736(14)61060-6).
 13. Hadinegoro SR, Arredondo-García JL, Capeding MR, Deseda C, Chotpitayasunondh T, Dietze R, Muhammad Ismail HI, Reynales H, Limkittikul K, Rivera-Medina DM. 2015. Efficacy and long-term safety of a dengue vaccine in regions of endemic disease. *N Engl J Med* 373:1195–1206. <https://doi.org/10.1056/NEJMoa1506223>.
 14. Halstead SB. 2017. Dengvaxia sensitizes seronegatives to vaccine enhanced disease regardless of age. *Vaccine* 35:6355–6358. <https://doi.org/10.1016/j.vaccine.2017.09.089>.
 15. Sanofi. 2017. Sanofi updates information on dengue vaccine. *Nasdaq Globe Newswire* https://www.sanofipasteur.com/media/Project/One-Sanofi-Web/sanofipasteur-com/en/media-room/docs/PR_20171129_SanofiUpdatesInfoOnDengueVaccine_EN.pdf.
 16. Kirkpatrick BD, Durbin AP, Pierce KK, Carmolli MP, Tibery CM, Grier PL, Hynes N, Diehl SA, Elwood D, Jarvis AP, Sabundayo BP, Lyon CE, Larsson CJ, Jo M, Lovchik JM, Luke CJ, Walsh MC, Fraser EA, Subbarao K, Whitehead SS. 2015. Robust and balanced immune responses to all 4 dengue virus serotypes following administration of a single dose of a live attenuated tetravalent dengue vaccine to healthy, flavivirus-naïve adults. *J Infect Dis* 212:702–710. <https://doi.org/10.1093/infdis/jiv082>.
 17. Roehrig JT, Bolin RA, Kelly RG. 1998. Monoclonal antibody mapping of the envelope glycoprotein of the dengue 2 virus, Jamaica. *Virology* 246:317–328. <https://doi.org/10.1006/viro.1998.9200>.
 18. Kuhn RJ, Zhang W, Rossmann MG, Pletnev SV, Corver J, Lenches E, Jones CT, Mukhopadhyay S, Chipman PR, Strauss EG. 2002. Structure of dengue virus: implications for flavivirus organization, maturation, and fusion. *Cell* 108:717–725. [https://doi.org/10.1016/S0092-8674\(02\)00660-8](https://doi.org/10.1016/S0092-8674(02)00660-8).
 19. Modis Y, Ogata S, Clements D, Harrison SC. 2003. A ligand-binding pocket in the dengue virus envelope glycoprotein. *Proc Natl Acad Sci U S A* 100:6986–6991. <https://doi.org/10.1073/pnas.0832193100>.
 20. Rey FA, Heinz FX, Mandl C, Kunz C, Harrison SC. 1995. The envelope glycoprotein from tick-borne encephalitis virus at 2 Å resolution. *Nature* 375:291–298. <https://doi.org/10.1038/375291a0>.
 21. Crill WD, Chang G-JJ. 2004. Localization and characterization of flavivirus envelope glycoprotein cross-reactive epitopes. *J Virol* 78:13975–13986. <https://doi.org/10.1128/JVI.78.24.13975-13986.2004>.
 22. Rouvinski A, Guardado-Calvo P, Barba-Spaeth G, Duquerroy S, Vanez M-C, Kikuti CM, Sanchez MEN, Dejnirattisai W, Wongwiwat W, Haouz A. 2015. Recognition determinants of broadly neutralizing human antibodies against dengue viruses. *Nature* 520:109–113. <https://doi.org/10.1038/nature14130>.
 23. Dejnirattisai W, Wongwiwat W, Supasa S, Zhang X, Dai X, Rouvinsky A, Jumnainsong A, Edwards C, Quyen NTH, Duangchinda T. 2015. A new class of highly potent, broadly neutralizing antibodies isolated from viremic patients infected with dengue virus. *Nat Immunol* 16:170–177. <https://doi.org/10.1038/ni.3058>.
 24. Crill WD, Roehrig JT. 2001. Monoclonal antibodies that bind to domain III of dengue virus E glycoprotein are the most efficient blockers of virus adsorption to Vero cells. *J Virol* 75:7769–7773. <https://doi.org/10.1128/JVI.75.16.7769-7773.2001>.
 25. Lok S-M, Kostyuchenko V, Nybakken GE, Holdaway HA, Battisti AJ, Sukupolvi-Petty S, Sedlak D, Fremont DH, Chipman PR, Roehrig JT. 2008. Binding of a neutralizing antibody to dengue virus alters the arrangement of surface glycoproteins. *Nature Struct Mol Biol* 15:312–317. <https://doi.org/10.1038/nsmb.1382>.
 26. Sukupolvi-Petty S, Austin SK, Purtha WE, Oliphant T, Nybakken GE, Schlesinger JJ, Roehrig JT, Gromowski GD, Barrett AD, Fremont DH. 2007. Type-and subcomplex-specific neutralizing antibodies against domain III of dengue virus type 2 envelope protein recognize adjacent epitopes. *J Virol* 81:12816–12826. <https://doi.org/10.1128/JVI.00432-07>.
 27. Cockburn JJ, Sanchez MEN, Fretes N, Urvoas A, Staropoli I, Kikuti CM, Coffey LL, Seisdedos FA, Bedouelle H, Rey FA. 2012. Mechanism of dengue virus broad cross-neutralization by a monoclonal antibody. *Structure* 20:303–314. <https://doi.org/10.1016/j.str.2012.01.001>.
 28. Tharakaraman K, Robinson LN, Hatas A, Chen Y-L, Siyue L, Raguram S, Sasisekharan V, Wogan GN, Sasisekharan R. 2013. Redesign of a cross-reactive antibody to dengue virus with broad-spectrum activity and increased in vivo potency. *Proc Natl Acad Sci U S A* 110:E1555–E1564. <https://doi.org/10.1073/pnas.1303645110>.
 29. Gromowski GD, Barrett AD. 2007. Characterization of an antigenic site that contains a dominant, type-specific neutralization determinant on the envelope protein domain III (ED3) of dengue 2 virus. *Virology* 366:349–360. <https://doi.org/10.1016/j.virol.2007.05.042>.
 30. Gromowski GD, Roehrig JT, Diamond MS, Lee JC, Pitcher TJ, Barrett AD. 2010. Mutations of an antibody binding energy hot spot on domain III of the dengue 2 envelope glycoprotein exploited for neutralization escape. *Virology* 407:237–246. <https://doi.org/10.1016/j.virol.2010.06.044>.
 31. Oliphant T, Engle M, Nybakken GE, Doane C, Johnson S, Huang L, Gorlatov S, Mehlhop E, Marri A, Chung KM. 2005. Development of a humanized monoclonal antibody with therapeutic potential against West Nile virus. *Nat Med* 11:522–530. <https://doi.org/10.1038/nm1240>.
 32. Nybakken GE, Oliphant T, Johnson S, Burke S, Diamond MS, Fremont DH. 2005. Structural basis of West Nile virus neutralization by a therapeutic antibody. *Nature* 437:764–769. <https://doi.org/10.1038/nature03956>.
 33. Megret F, Hugnot J, Falconar A, Gentry M, Morens D, Murray J, Schlesinger J, Wright P, Young P, Van Regenmortel M. 1992. Use of recombinant fusion proteins and monoclonal antibodies to define linear and discontinuous antigenic sites on the dengue virus envelope glycoprotein. *Virology* 187:480–491. [https://doi.org/10.1016/0042-6822\(92\)90450-4](https://doi.org/10.1016/0042-6822(92)90450-4).
 34. Robinson LN, Tharakaraman K, Rowley KJ, Costa VV, Chan KR, Wong YH, Ong LC, Tan HC, Koch T, Cain D. 2015. Structure-guided design of an anti-dengue antibody directed to a non-immunodominant epitope. *Cell* 162:493–504. <https://doi.org/10.1016/j.cell.2015.06.057>.
 35. Simmons M, Murphy GS, Hayes CG. 2001. Short report: Antibody responses of mice immunized with a tetravalent dengue recombinant protein subunit vaccine. *Am J Trop Med Hyg* 65:159–161. <https://doi.org/10.4269/ajtmh.2001.65.159>.
 36. Simmons M, Nelson WM, Wu S, Hayes CG. 1998. Evaluation of the protective efficacy of a recombinant dengue envelope B domain fusion protein against dengue 2 virus infection in mice. *Am J Trop Med Hyg* 58:655–662. <https://doi.org/10.4269/ajtmh.1998.58.655>.
 37. Hermida L, Bernardo L, Martín J, Alvarez M, Prado I, López C, Sierra BDL, Martínez CR, Rodríguez R, Zulueta A. 2006. A recombinant fusion protein containing the domain III of the dengue-2 envelope protein is immunogenic and protective in nonhuman primates. *Vaccine* 24:3165–3171. <https://doi.org/10.1016/j.vaccine.2006.01.036>.
 38. Hermida L, Rodríguez R, Lazo L, Silva R, Zulueta A, China G, López C, Guzmán MG, Guillén G. 2004. A dengue-2 envelope fragment inserted within the structure of the P64k meningococcal protein carrier enables a functional immune response against the virus in mice. *J Virol Methods* 115:41–49. <https://doi.org/10.1016/j.jviromet.2003.09.024>.
 39. Saejung W, Fujiyama K, Takasaki T, Ito M, Hori K, Malasit P, Watanabe Y, Kurane I, Seki T. 2007. Production of dengue 2 envelope domain III in plant using TMV-based vector system. *Vaccine* 25:6646–6654. <https://doi.org/10.1016/j.vaccine.2007.06.029>.
 40. Zhang Z-S, Yan Y-S, Weng Y-W, Huang H-L, Li S-Q, He S, Zhang J-M. 2007. High-level expression of recombinant dengue virus type 2 envelope domain III protein and induction of neutralizing antibodies in BALB/C mice. *J Virol Methods* 143:125–131. <https://doi.org/10.1016/j.jviromet.2007.02.012>.
 41. Chin J, Chu J, Ng M. 2007. The envelope glycoprotein domain III of

- dengue virus serotypes 1 and 2 inhibit virus entry. *Microbes Infect* 9:1–6. <https://doi.org/10.1016/j.micinf.2006.09.009>.
42. Batra G, Raut R, Dahiya S, Kamran N, Swaminathan S, Khanna N. 2010. Pichia pastoris-expressed dengue virus type 2 envelope domain III elicits virus-neutralizing antibodies. *J Virol Methods* 167:10–16. <https://doi.org/10.1016/j.jviromet.2010.03.002>.
 43. Simmons M, Porter KR, Hayes CG, Vaughn DW, Putnak R. 2006. Characterization of antibody responses to combinations of a dengue virus type 2 DNA vaccine and two dengue virus type 2 protein vaccines in rhesus macaques. *J Virol* 80:9577–9585. <https://doi.org/10.1128/JVI.00284-06>.
 44. Bernardo L, Hermida L, Martin J, Alvarez M, Prado I, López C, Martínez R, Rodríguez-Roche R, Zulueta A, Lazo L. 2008. Anamnestic antibody response after viral challenge in monkeys immunized with dengue 2 recombinant fusion proteins. *Arch Virol* 153:849–854. <https://doi.org/10.1007/s00705-008-0050-9>.
 45. Bernardo L, Izquierdo A, Alvarez M, Rosario D, Prado I, López C, Martínez R, Castro J, Santana E, Hermida L. 2008. Immunogenicity and protective efficacy of a recombinant fusion protein containing the domain III of the dengue 1 envelope protein in non-human primates. *Antivir Res* 80:194–199. <https://doi.org/10.1016/j.antiviral.2008.06.005>.
 46. Li X-Q, Qiu L-W, Chen Y, Wen K, Cai J-P, Chen J, Pan Y-X, Li J, Hu D-M, Huang Y-F. 2013. Dengue virus envelope domain III immunization elicits predominantly cross-reactive, poorly neutralizing antibodies localized to the AB loop: implications for dengue vaccine design. *J Gen Virol* 94:2191–2201. <https://doi.org/10.1099/vir.0.055178-0>.
 47. Midgley CM, Flanagan A, Tran HB, Dejnirattisai W, Chawansuntati K, Jumnainsong A, Wongwiwat W, Duangchinda T, Mongkolsapaya J, Grimes JM. 2012. Structural analysis of a dengue cross-reactive antibody complexed with envelope domain III reveals the molecular basis of cross-reactivity. *J Immunol* 188:4971–4979. <https://doi.org/10.4049/jimmunol.1200227>.
 48. Zhao H, Fernandez E, Dowd KA, Speer SD, Platt DJ, Gorman MJ, Govero J, Nelson CA, Pierson TC, Diamond MS. 2016. Structural basis of Zika virus-specific antibody protection. *Cell* 166:1016–1027. <https://doi.org/10.1016/j.cell.2016.07.020>.
 49. Gentry M, Henchal E, McCown J, Brandt W, Dalrymple J. 1982. Identification of distinct antigenic determinants on dengue-2 virus using monoclonal antibodies. *Am J Trop Med Hyg* 31:548–555. <https://doi.org/10.4269/ajtmh.1982.31.548>.
 50. Henchal E, McCown J, Burke D, Seguin M, Brandt W. 1985. Epitopic analysis of antigenic determinants on the surface of dengue-2 virions using monoclonal antibodies. *Am J Trop Med Hyg* 34:162–169. <https://doi.org/10.4269/ajtmh.1985.34.162>.
 51. Correia BE, Bates JT, Loomis RJ, Baneyx G, Carrico C, Jardine JG, Rupert P, Correnti C, Kalyuzhnyi O, Vittal V. 2014. Proof of principle for epitope-focused vaccine design. *Nature* 507:201–206. <https://doi.org/10.1038/nature12966>.
 52. Delves PJ, Lund T, Roitt IM. 1997. Can epitope-focused vaccines select advantageous immune response? *Mol Med Today* 3:55–60. [https://doi.org/10.1016/S1357-4310\(96\)20036-X](https://doi.org/10.1016/S1357-4310(96)20036-X).
 53. Chiesa MD, Martensen PM, Simmons C, Porakishvili N, Justesen J, Dougan G, Roitt IM, Delves PJ, Lund T. 2001. Refocusing of B-cell responses following a single amino acid substitution in an antigen. *Immunology* 103:172–178. <https://doi.org/10.1046/j.1365-2567.2001.01242.x>.
 54. Wu X, Yang Z-Y, Li Y, HogerCorp C-M, Schief WR, Seaman MS, Zhou T, Schmidt SD, Wu L, Xu L. 2010. Rational design of envelope identifies broadly neutralizing human monoclonal antibodies to HIV-1. *Science* 329:856–861. <https://doi.org/10.1126/science.1187659>.
 55. Impagliazzo A, Milder F, Kuipers H, Wagner MV, Zhu X, Hoffman RM, van Meersbergen R, Huizingh J, Wannings P, Verspuij J, de Man M, Ding Z, Apetri A, Kukrer B, Sneekes-Vriese E, Tomkiewicz D, Laursen NS, Lee PS, Zakrzewska A, Dekking L, Tolboom J, Tettero L, van Meerten S, Yu W, Koudstaal W, Goudsmit J, Ward AB, Meijberg W, Wilson IA, Radosevic K. 2015. A stable trimeric influenza hemagglutinin stem as a broadly protective immunogen. *Science* 349:1301–1306. <https://doi.org/10.1126/science.aac7263>.
 56. Kulp DW, Steichen JM, Pauthner M, Hu X, Schiffner T, Liguori A, Cottrell CA, Havenar-Daughton C, Ozorowski G, Georgeson E, Kalyuzhnyi O, Willis JR, Kubitz M, Adachi Y, Reiss SM, Shin M, de Val N, Ward AB, Crotty S, Burton DR, Schief WR. 2017. Structure-based design of native-like HIV-1 envelope trimers to silence non-neutralizing epitopes and eliminate CD4 binding. *Nat Commun* 8:1655. <https://doi.org/10.1038/s41467-017-01549-6>.
 57. Rubinstein ND, Mayrose I, Halperin D, Yekutieli D, Gershoni JM, Pupko T. 2008. Computational characterization of B-cell epitopes. *Mol Immunol* 45:3477–3489. <https://doi.org/10.1016/j.molimm.2007.10.016>.
 58. Block OK, Rodrigo WSI, Quinn M, Jin X, Rose RC, Schlesinger JJ. 2010. A tetravalent recombinant dengue domain III protein vaccine stimulates neutralizing and enhancing antibodies in mice. *Vaccine* 28:8085–8094. <https://doi.org/10.1016/j.vaccine.2010.10.004>.
 59. Frei JC, Kielian M, Lai JR. 2015. Comprehensive mapping of functional epitopes on dengue virus glycoprotein E DIII for binding to broadly neutralizing antibodies 4E11 and 4E5A by phage display. *Virology* 485:371–382. <https://doi.org/10.1016/j.virol.2015.08.011>.
 60. Sidhu SS, Geyer CR. 2015. Phage display in biotechnology and drug discovery. CRC Press, Boca Raton, FL.
 61. Koide A, Wojcik J, Gilbreth RN, Hoey RJ, Koide S. 2012. Teaching an old scaffold new tricks: monoclonal antibodies constructed using alternative surfaces of the FN3 scaffold. *J Mol Biol* 415:393–405. <https://doi.org/10.1016/j.jmb.2011.12.019>.
 62. Sidhu SS, Lowman HB, Cunningham BC, Wells JA. 2000. Phage display for selection of novel binding peptides. *Methods Enzymol* 328:333. [https://doi.org/10.1016/S0076-6879\(00\)28406-1](https://doi.org/10.1016/S0076-6879(00)28406-1).
 63. Saff E, Kuijlaars A. 1997. AREAIMOL. *Mathematical Intelligencer* 19:5–11.
 64. Lee B, Richards FM. 1971. The interpretation of protein structures: estimation of static accessibility. *J Mol Biol* 55:379–400. [https://doi.org/10.1016/0022-2836\(71\)90324-X](https://doi.org/10.1016/0022-2836(71)90324-X).
 65. Jackson RM. 1999. Comparison of protein-protein interactions in serine protease-inhibitor and antibody-antigen complexes: implications for the protein docking problem. *Protein Sci* 8:603–613. <https://doi.org/10.1110/ps.8.3.603>.
 66. Frei JC, Lai JR. 2016. Protein and antibody engineering by phage display. *Methods Enzymol* 580:45–87. <https://doi.org/10.1016/bs.mie.2016.05.005>.
 67. Preiner J, Kodera N, Tang J, Ebner A, Brameshuber M, Blaas D, Gelbmann N, Gruber HJ, Ando T, Hinterdorfer P. 2014. IgGs are made for walking on bacterial and viral surfaces. *Nat Commun* 5:4394. <https://doi.org/10.1038/ncomms5394>.
 68. Huang KC, Lee MC, Wu CW, Huang KJ, Lei HY, Cheng JW. 2008. Solution structure and neutralizing antibody binding studies of domain III of the dengue-2 virus envelope protein. *Proteins* 70:1116–1119. <https://doi.org/10.1002/prot.21806>.
 69. Johnson AJ, Roehrig JT. 1999. New mouse model for dengue virus vaccine testing. *J Virol* 73:783–786.
 70. Zulueta A, Martín J, Hermida L, Alvarez M, Valdés I, Prado I, China G, Rosario D, Guillén G, Guzmán MG. 2006. Amino acid changes in the recombinant dengue 3 envelope domain III determine its antigenicity and immunogenicity in mice. *Virus Res* 121:65–73. <https://doi.org/10.1016/j.virusres.2006.04.003>.
 71. Capra JD, Janeway CA, Travers P, Walport M. 1999. Immunobiology: the immune system in health and disease. Garland Publishing, New York, NY.
 72. Balsitis SJ, Williams KL, Lachica R, Flores D, Kyle JL, Mehlhop E, Johnson S, Diamond MS, Beatty PR, Harris E. 2010. Lethal antibody enhancement of dengue disease in mice is prevented by Fc modification. *PLoS Pathog* 6:e1000790. <https://doi.org/10.1371/journal.ppat.1000790>.
 73. Zellweger RM, Prestwood TR, Shresta S. 2010. Antibodies enhance infection of LSECs in a model of ADE-induced severe dengue disease. *Cell Host Microbe* 7:128–139. <https://doi.org/10.1016/j.chom.2010.01.004>.
 74. Marcos E, Gil L, Lazo L, Izquierdo A, Brown E, Suzarte E, Valdés I, García A, Méndez L, Guzmán MG. 2013. Purified and highly aggregated chimeric protein DIII-2 induces a functional immune response in mice against dengue 2 virus. *Arch Virol* 158:225–230. <https://doi.org/10.1007/s00705-012-1471-z>.
 75. Valdés I, Bernardo L, Gil L, Pavón A, Lazo L, López C, Romero Y, Menéndez I, Falcón V, Betancourt L. 2009. A novel fusion protein domain III-capsid from dengue-2, in a highly aggregated form, induces a functional immune response and protection in mice. *Virology* 394:249–258. <https://doi.org/10.1016/j.virol.2009.08.029>.
 76. Etamad B, Batra G, Raut R, Dahiya S, Khanam S, Swaminathan S, Khanna N. 2008. An envelope domain III-based chimeric antigen produced in Pichia pastoris elicits neutralizing antibodies against all four dengue virus serotypes. *Am J Trop Med Hyg* 79:353–363.
 77. Leng C-H, Liu S-J, Tsai J-P, Li Y-S, Chen M-Y, Liu H-H, Lien S-P, Yueh A, Hsiao K-N, Lai L-W. 2009. A novel dengue vaccine candidate that induces cross-neutralizing antibodies and memory immunity. *Microbes Infect* 11:288–295. <https://doi.org/10.1016/j.micinf.2008.12.004>.
 78. Bardina SV, Bunduc P, Tripathi S, Duehr J, Frere JJ, Brown JA, Nachbagauer R, Foster GA, Krysztof D, Tortorella D, Stramer SL, Garcia-Sastre

- A, Krammer F, Lim JK. 2017. Enhancement of Zika virus pathogenesis by preexisting antinflavivirus immunity. *Science* 356:175–180. <https://doi.org/10.1126/science.aal4365>.
79. Dejnirattisai W, Supasa P, Wongwiwat W, Rouvinski A, Barba-Spaeth G, Duangchinda T, Sakuntabhai A, Cao-Lormeau V-M, Malasit P, Rey FA. 2016. Dengue virus sero-cross-reactivity drives antibody-dependent enhancement of infection with Zika virus. *Nat Immunol* 17:1102–1108. <https://doi.org/10.1038/ni.3515>.
80. Paul LM, Carlin ER, Jenkins MM, Tan AL, Barcellona CM, Nicholson CO, Michael SF, Isern S. 2016. Dengue virus antibodies enhance Zika virus infection. *Clin Transl Immunology* 5:e117. <https://doi.org/10.1038/cti.2016.72>.
81. Priyamvada L, Quicke KM, Hudson WH, Onlamoon N, Sewatanon J, Edupuganti S, Pattanapanyasat K, Chokeyhaibulkit K, Mulligan MJ, Wilson PC. 2016. Human antibody responses after dengue virus infection are highly cross-reactive to Zika virus. *Proc Natl Acad Sci U S A* 113:7852–7857. <https://doi.org/10.1073/pnas.1607931113>.
82. Stettler K, Beltramello M, Espinosa DA, Graham V, Cassotta A, Bianchi S, Vanzetta F, Minola A, Jaconi S, Mele F. 2016. Specificity, cross-reactivity and function of antibodies elicited by Zika virus infection. *Science* 353:823–826. <https://doi.org/10.1126/science.aaf8505>.
83. Slon Campos JL, Poggianella M, Marchese S, Mossenta M, Rana J, Arnoldi F, Bestagno M, Burrone OR. 2017. DNA-immunisation with dengue virus E protein domains I/II, but not domain III, enhances Zika, West Nile and Yellow Fever virus infection. *PLoS One* 12:e0181734. <https://doi.org/10.1371/journal.pone.0181734>.
84. Wengler G. 1989. Cell-associated West Nile flavivirus is covered with E+pre-M protein heterodimers which are destroyed and reorganized by proteolytic cleavage during virus release. *J Virol* 63:2521–2526.
85. Marley J, Lu M, Bracken C. 2001. A method for efficient isotopic labeling of recombinant proteins. *J Biomol NMR* 20:71–75. <https://doi.org/10.1023/A:1011254402785>.
86. Orekhov VY, Jaravine VA. 2011. Analysis of non-uniformly sampled spectra with multi-dimensional decomposition. *Prog Nucl Magn Reson Spectrosc* 59:271–292. <https://doi.org/10.1016/j.pnmrs.2011.02.002>.
87. Delaglio F, Grzesiek S, Vuister GW, Zhu G, Pfeifer J, Bax A. 1995. NMRPipe: a multidimensional spectral processing system based on UNIX pipes. *J Biomol NMR* 6:277–293. <https://doi.org/10.1007/BF00197809>.
88. Vranken WF, Boucher W, Stevens TJ, Fogh RH, Pajon A, Llinas M, Ulrich EL, Markley JL, Ionides J, Laue ED. 2005. The CCPN data model for NMR spectroscopy: development of a software pipeline. *Proteins* 59:687–696. <https://doi.org/10.1002/prot.20449>.
89. Brien JD, Austin SK, Sukupolvi-Petty S, O'Brien KM, Johnson S, Fremont DH, Diamond MS. 2010. Genotype-specific neutralization and protection by antibodies against dengue virus type 3. *J Virol* 84:10630–10643. <https://doi.org/10.1128/JVI.01190-10>.
90. Dowd KA, Mukherjee S, Kuhn RJ, Pierson TC. 2014. Combined effects of the structural heterogeneity and dynamics of flaviviruses on antibody recognition. *J Virol* 88:11726–11737. <https://doi.org/10.1128/JVI.01140-14>.